Cardiology

Thrombocardiology

Cardiology
DOI: 10.1159/000548375

Received: June 23, 2025
Accepted: September 3, 2025
Published online: September 9, 2025

In vitro and ex vivo Flow Models for Arterial Thrombosis: A Systematic Review

Hande Eyisoylu[a] Rachele Cagnazzo[b] Gijsje H. Koenderink[c]
Moniek P.M. de Maat[a] Heleen M.M. van Beusekom[b]

[a]Department of Hematology, Erasmus MC Cardiovascular Institute, Erasmus MC University Medical Center Rotterdam, Rotterdam, The Netherlands; [b]Department of Cardiology, Erasmus MC Cardiovascular Institute, Erasmus MC University Medical Center Rotterdam, Rotterdam, The Netherlands; [c]Department of Bionanoscience, Kavli Institute of Nanoscience, Delft University of Technology, Delft, The Netherlands

Keywords
Arterial thrombosis · In vitro models · Ex vivo models · Microfluidics · Shear stress

Abstract
Introduction: Arterial thrombosis is a multifaceted process characterized by platelet aggregation and fibrin deposition, leading to the occlusion of blood vessels. It plays a central role in cardiovascular conditions such as myocardial infarction and ischemic stroke. Gaining insight into the mechanisms underlying arterial thrombosis is essential for developing effective treatments aimed at preventing thrombotic events and reducing associated health burdens. In vitro and ex vivo models serve as critical tools for investigating the pathophysiology of arterial thrombosis by providing controlled environments to study thrombus formation and characteristics. This systematic review provides a comprehensive overview of in vitro and ex vivo flow-based models used to study arterial thrombosis, classifying them by scale (macro vs. micro) and evaluating their design principles, physiological relevance, and experimental utility. ***Methods:*** A systematic search of Medline, Embase, and Web of Science was conducted using broad and specific terms related to arterial thrombosis models incorporating flow or shear stress. Articles were screened by two independent reviewers. Studies were included if they described in vitro or ex vivo models with dynamic flow; models limited to static or venous conditions or in vivo studies were excluded. In total, 82 studies met the inclusion criteria. ***Results:*** Macro-scale models can mimic complex flow patterns in larger arterial conditions and enable the formation of thrombi comparable in size to clinical specimens. Microfluidic models allow precise control over shear conditions and geometry with minimal blood volumes and are suitable for high-resolution imaging and customization, including endothelialization and patient-specific designs. While, both model types present limitations in replicating complex in vivo hemodynamics, standardization, and scalability, they offer valuable, controllable platforms for mechanistic studies and drug testing in arterial thrombosis. ***Conclusions:*** While no single model fully recapitulates the in vivo

Hande Eyisoylu and Rachele Cagnazzo share first authorship.
Moniek P.M. de Maat and Heleen M.M. van Beusekom share last authorship.

karger@karger.com
www.karger.com/crd

Karger
OPEN ACCESS

Correspondence to:
Heleen M.M. van Beusekom, h.vanbeusekom@erasmusmc.nl

environment, ongoing innovations, particularly in microfabrication and model standardization, continue to improve physiological relevance and clinical translatability.

Introduction

Arterial thrombosis, a complex process involving platelet aggregation and fibrin deposition that leads to vessel occlusion, is a pathological event underlying cardiovascular diseases such as myocardial infarction and ischemic stroke [1]. Understanding the mechanisms governing arterial thrombosis is crucial for the development of effective therapies to prevent thrombotic events and mitigate associated morbidity and mortality. The initiation and propagation of arterial thrombosis are linked to atherosclerosis, an inflammatory condition characterized by the accumulation of lipids, immune cells, and a formation of a fibrous plaque within the arterial wall, causing a stenosis which disturbs the blood flow [1, 2]. Rupture or erosion of these atherosclerotic plaques exposes prothrombotic components, such as tissue factor and collagen, triggering platelet activation and the coagulation cascade, ultimately leading to thrombus formation [1, 2].

In vitro and ex vivo models play a pivotal role in unraveling the pathophysiology of arterial thrombosis, offering controlled experimental settings for investigating the formation and properties of thrombi. In this review, we define in vitro models as models in which freshly drawn blood or plasma is perfused or circulated through artificial channels, tubes, or over biologically coated surfaces, without the use of intact native tissues. Ex vivo models are defined here as systems in which blood is either circulated directly from the patient or blood is perfused over a native vascular tissue, preserving both biological architecture and physiological flow – a criterion met only by the Badimon chamber among the models reviewed. These models are essential in complementing in vivo studies, which, while valuable, are limited by species differences, variability in disease progression, challenges in real-time observation and manipulation, and ethical considerations [3]. Both in vitro and ex vivo platforms offer advantages, such as precise control over experimental variables, reproducibility, patient specificity, and the ability to dissect cellular and molecular mechanisms of thrombus formation [4]. Moreover, these models offer the flexibility to simulate various aspects of the arterial microenvironment. This includes hemodynamic forces, vessel geometry, and interactions with circulating blood components, thereby recapitulating key features of thrombus formation in vivo [4].

Over the past decades, significant advancements have been made in the development of both in vitro and ex vivo arterial thrombosis models, especially driven by innovations in microfluidic technologies and perfusion systems [4–7]. In vivo, blood flow is an essential component of arterial thrombosis formation and propagation. Flow exerts shear forces on circulating platelets and influences thrombosis via von Willebrand factor stretching and fibrin network organization [8]. Therefore, both in vitro and ex vivo models that incorporate flow conditions play a pivotal role in mimicking the dynamic nature of arterial thrombosis and studying its modulation by shear stress and flow patterns.

In this review, we provide a comprehensive overview of the current state-of-the-art in vitro and ex vivo arterial thrombosis models that incorporate the influence of blood flow. In the context of this review, we use the term flow to encompass not only the active perfusion of blood through channels or tubing, but also systems that apply dynamic mechanical forces – such as rotational shear or oscillation – to stimulate thrombus formation under physiologically relevant and dynamic conditions. To facilitate a clear comparison among models, we have classified the in vitro and ex vivo models identified in our search results into two categories: macro-scaled and micro-scaled models. Macro-scaled models operate within dimensions ranging from millimeters to centimeters and require relatively large volumes of blood (often milliliters), whereas micro-scaled models function at the micrometer scale and require smaller blood volumes (mL) for thrombus formation. We discuss the principles underlying the design of in vitro and ex vivo arterial thrombosis models and highlight their respective strengths and limitations in mimicking the complex physiological environment of arterial thrombosis. Finally, we outline key parameters that should be reported to promote standardization and reproducibility in experimental studies utilizing in vitro and ex vivo models of arterial thrombosis.

Methods and Selection Criteria

To guide our study selection, we adopted a Sample, Phenomenon of Interest, Design, Evaluation, Research type (SPIDER) framework, suitable for qualitative and mixed-methods reviews. Our review was driven by the following research question:

What are the available in vitro and ex vivo arterial thrombosis models that incorporate flow or shear stress, and how do they compare in terms of physiological relevance, reproducibility, and translational applicability?

This question informed our inclusion and exclusion criteria as follows.

- Sample (S): Studies involving human or animal-derived whole blood, plasma, or platelets used in in vitro or ex vivo thrombosis models. Studies using only purified components (e.g., fibrinogen alone) or non-blood analogs were excluded.
- Phenomenon of interest (PI): Models that simulate arterial thrombosis under flow or shear stress conditions. Only studies that assessed dynamic thrombus formation were included. We excluded models limited to static conditions or designed for or employed specifically venous thrombosis.
- Design (D): Original experimental studies using in vitro or ex vivo flow models, including macrofluidic, microfluidic, or perfusion systems. In vivo animal models, static assays, and computational-only simulations were excluded.
- Evaluation (E): Studies that reported and therefore allowed assessment of model performance, physiological relevance, flow parameters, or thrombus characterization (e.g., size, composition, formation time).
- Research type (R): Peer-reviewed original research articles. We excluded conference abstracts, reviews, commentaries, and studies not published in English. Articles without accessible full text were also excluded.

All search terms included "thrombosis models," which was combined with other search terms, including ex vivo, in vitro, arterial thrombosis, Chandler loop, Modified Chandler loop, Roller pump, Ball valve circulation model, Thrombosis-on-a-chip, Microfluidic-based models, Parallel plate viscomet*, Parallel plate rheomet*, Cone and plate viscomet*, Cone and plate rheomet*, Flow chamber, Flat plate flow chamber, Parallel plate flow chamber, Flow loop, TEG, ROTEM, Microfluidic devices (full search term can be found in the online suppl. material along with the PRISMA checklist; for all online suppl. material, see https://doi.org/10.1159/000548375). No restriction was placed on publication date and models should include either flow or the proxy shear stress. In vivo models were excluded. Venous thrombosis models and models that enable the formation of thrombi under static conditions were also excluded.

After deduplication, the first search resulted in 2784 articles. The systematic search was conducted on April 13, 2023, and article screening was performed independently by two researchers throughout April 2023. The first selection was made based on title and abstract, 2,619 were excluded at this round and 165 were selected for full-text screening. Initially, 70 articles were included in this systematic review. An updated search using the same strategy was performed on April 29, 2025, identifying 495 additional articles (post-deduplication). After title/abstract and full-text screening, 12 additional studies were included.

In total, 82 studies were included in this review. Articles were excluded if they did not address the research question, were not in English, lacked full text, or were reviews or conference abstracts. The full inclusion process is shown in Figure 1.

Results

Following the classification by model scale introduced earlier, we first describe macro-scaled models, followed by micro-scaled models. Macro-scaled models include tubing or chambers with diameters ranging from millimeters to centimeters and require larger volumes of blood (often milliliters) whereas micro-scaled models operate within micrometer dimensions (in terms of diameter, width, and/or length) and require a smaller blood volume (mL) for thrombus formation. To quantitatively compare the flow characteristics among different models, shear rate or stress and several dimensionless numbers are typically used (see Table 1).

Macrofluidic Models

To investigate how controlled shear conditions influence thrombus formation, macrofluidic models provide a valuable platform, particularly for studying blood-material interactions under well-defined hemodynamic environments. Among the earliest macrofluidic approaches are the cone-and-plate and two-disc rheometers (Fig. 2), which remain in use for specific applications. In a cone-and-plate system, a cone rotates atop a flat plate, generating a uniform shear rate across the surface – a key advantage for reproducible measurements. In contrast, the two-disc (or plate-plate) system produces a radial shear gradient, where the shear rate increases with distance from the center. Although this introduces variability, it offers practical benefits, such as adjustable gap height between the plates, allowing greater flexibility in experimental design. These models

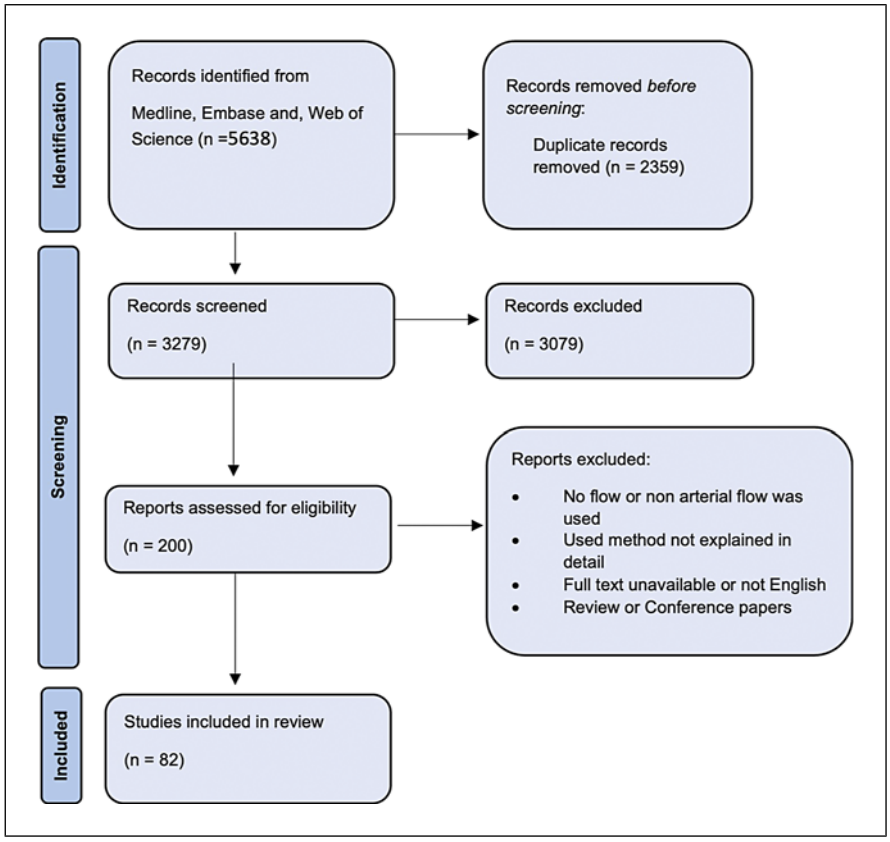

Fig. 1. Flowchart of inclusion and exclusion methods.

have historically been used to study the effects of shear stress on platelets and endothelial cells [5, 9, 10], and continue to be relevant for foundational mechanistic studies in thrombosis research.

Chandler Loop

The Chandler Loop is an in vitro method for generating thrombi by rotating citrated blood or plasma in a rotating tube to simulate in vivo flow conditions [11, 12]. Although there is no true unidirectional flow, movement of blood occurs due to rotation, gravitational effects, shear from tube motion, and the presence of an air bubble, which remains at the highest point and contributes to internal recirculation (Fig. 3a). This setup mimics certain aspects of physiological hemodynamics, such as arterial curvature and bifurcation [13]. Coagulation is typically initiated by adding $CaCl_2$ and/or thrombin. Tubes are rotated at 15–40 RPM (revolutions per minute) for up to 90 min at room temperature or at 37°C, simulating arterial shear rates of ~400–600 s^{-1} (Table 2) [13–17].

A computational study on the flow physics within the Chandler Loop by Touma et al. [18] demonstrated that the flow within the loop is highly complex, with non-uniform velocity and strain rate fields. Structurally, thrombi formed in the Chandler Loop show a white, platelet-rich head and a red tail, visually resembling patient arterial thrombi [19] though quantitative comparisons remain limited. The model is valued for its simplicity, yet lacks standardization, with variation in tube dimensions, RPM, angle, and temperature across studies. Limitations include restricted shear control, and at higher speeds, the air bubble may rotate with the blood, disrupting the intended flow pattern [20, 21]. While it can replicate artery-sized tubing, the flow pattern is complex and difficult to characterize, requiring a relatively large volume of blood (about 3 mL) to fill the tubing for desired flow rates.

Modified Chandler Loop

Variations of the Chandler Loop – termed "Modified Chandler Loops" – replace the standard PVC tubing with vascular devices such as stents, heart valves, or catheters to assess thrombus formation on clinically relevant materials [22–24]. These models may also include connectors or infusion ports for fluid exchange and allow adjustment of device positioning, including catheter

Table 1. Brief explanations of flow parameters which provide guidance for designing flow models so that they mimic in vivo flow conditions during arterial thrombosis

Flow parameter	Meaning	Units/how calculated
Dimensional parameters		
Shear rate (γ)	Rate of fluid deformation at the wall; governs platelet transport and activation thresholds. Typical arterial ranges ≈ 300–2,000 s^{-1} in straight segments; can exceed 5,000–10,000 s^{-1} in stenoses	Units: s^{-1}. Circular tube: γ_w ≈ 8U/D (U = mean velocity, D = diameter). Parallel-plate/rectangular with w≫h: γ_w ≈ 6Q/(w·h^2) (Q = flow rate, w = width, h = height)
Wall shear stress (τ_w)	Tangential stress exerted by blood on the wall; influences platelet/vWF activation. At arterial conditions, whole blood behaves quasi-Newtonian	Units: Pa (1 Pa = 10 dyn·cm^{-2}). τ_w = μ·γ_w
Dimensionless numbers		
Reynolds number (Re)	Determines the type of flow pattern (laminar vs. turbulent). Ratio of inertial to viscous forces; indicates flow regime. Pipe rule-of-thumb: Re ≲ 2,000 laminar; higher values approach transitional/turbulent. Microfluidic channels typically have Re < 1 due to small length scales	Re = ρ·U·L/μ (or U·D/ν in pipes). Report characteristic length (L or D) and how U was obtained
Péclet number (Pe)	Relative importance of advection vs. diffusion for solute transport. Pe ≫ 1: advection-dominated; Pe ≪ 1: diffusion-dominated near reaction site	Pe = U·L/D_m (D_m = molecular diffusivity). Also Pe = Re·Sc, where Sc = ν/D_m
Damköhler number (Da)	Relative importance of reaction vs. transport. Da ≫ 1: reaction faster than transport (transport-limited); Da ≪ 1: transport faster (reaction-limited)	Specify definition used. Advection-based: Da_I = k·L/U. Diffusion-based: Da_II = k·L^2/D_m (k = effective reaction rate constant)

γ, shear rate (s^{-1}); γ_w, wall shear rate (s^{-1}); τ_w, wall shear stress (pa); μ, dynamic viscosity (pa·s); ν, kinematic viscosity ($m^2 \cdot s^{-1}$ = μ/ρ); ρ, fluid density ($kg \cdot m^{-3}$); u, mean/bulk velocity ($m \cdot s^{-1}$); q, volumetric flow rate ($m^3 \cdot s^{-1}$); d, tube inner diameter (m); w, channel width (m); h, channel height (m); l, characteristic length – pipe diameter or hydraulic diameter (m); d_m, molecular diffusivity ($m^2 \cdot s^{-1}$); k, effective reaction rate constant (s^{-1}); Re, Reynolds number (ρul/μ or ud/ν); Pe, Péclet number (ul/d_m = re·sc); Sc, Schmidt number (ν/d_m); Da, Damköhler number (Da_I = kl/u, Da_{ii} = kl^2/d_m). Pa, pascal; dyn·cm^{-2}, dyne per square centimeter (1 pa = 10 dyn·cm^{-2}).

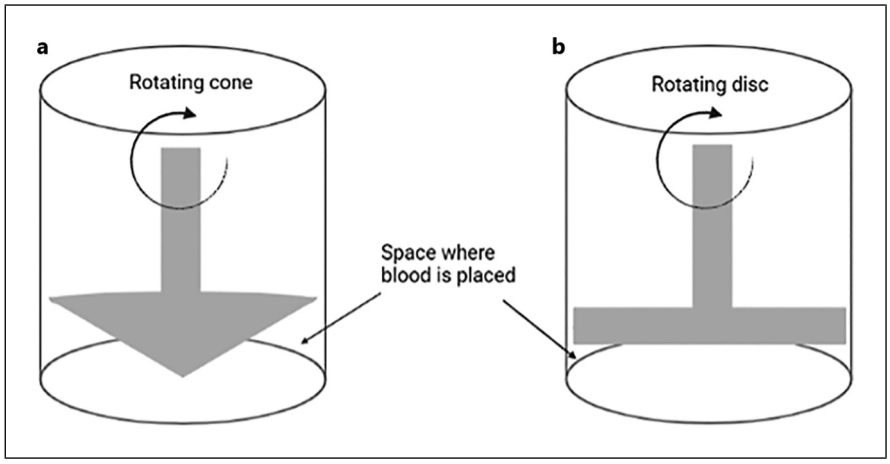

Fig. 2. Simplified representation of rheometric systems used in macrofluidic thrombosis models. **a** Cone-and-plate rheometer: a conical spindle rotates over a flat plate with a small angle, generating defined shear stress. **b** Two-disc rheometer: two parallel rotating discs simulate shear conditions between surfaces. These illustrations are schematic and not drawn to scale. Typical plate diameters are in the cm-range and typical gaps are in the range of several 100 μm. Images adapted from [90].

orientation. Thrombogenicity is typically evaluated via plasma markers or thrombus weight, though the latter provides limited mechanistic detail. Some studies report a more physiological flow conditions [21], but details on how these are achieved are often lacking. The term "modified Chandler Loop" is inconsistently used in the

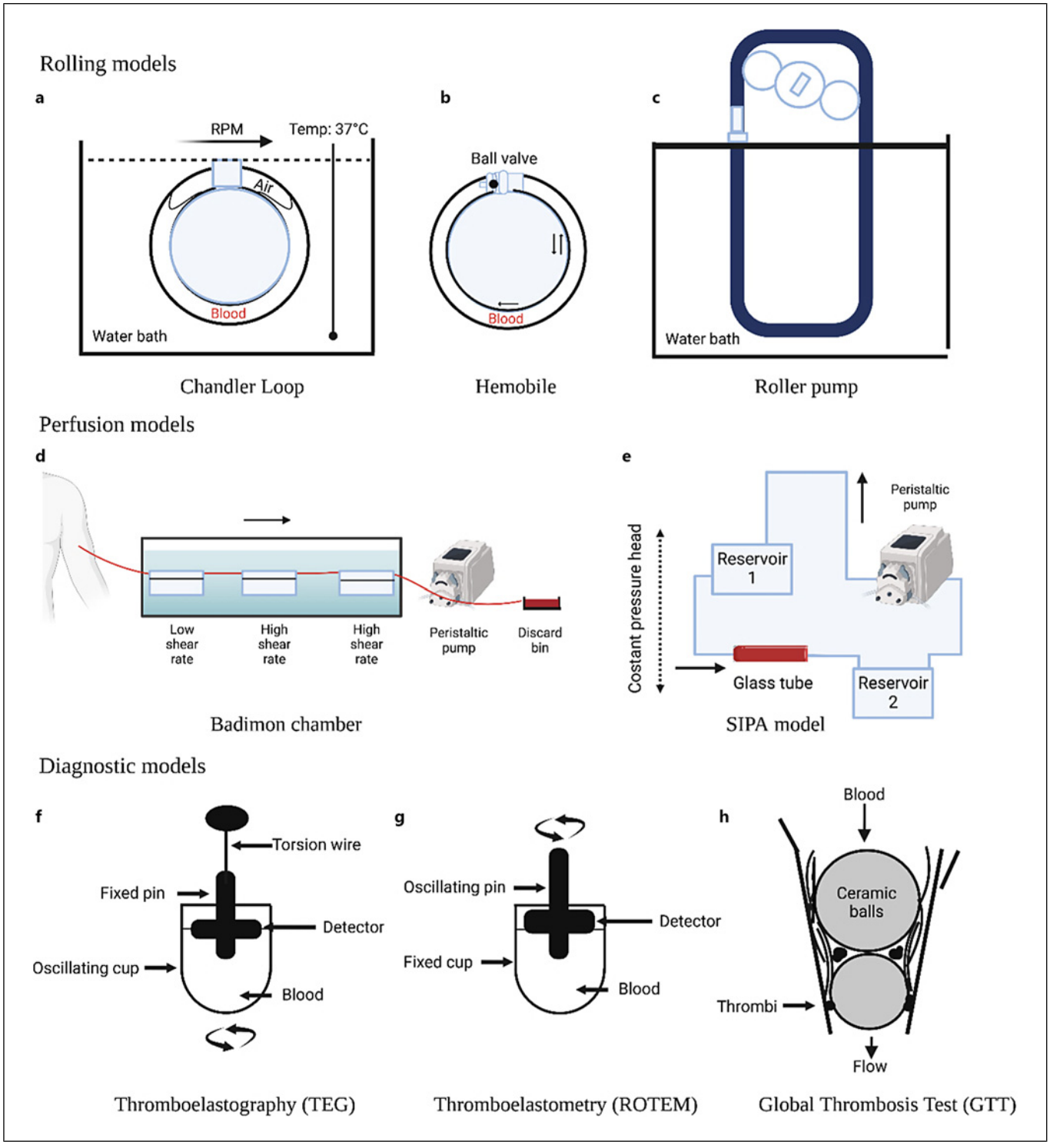

3

(For legend see next page.)

literature, with limited reporting on key parameters such as tubing dimensions, rotation speed, and temperature. This lack of standardization hampers reproducibility and cross-study comparison.

Ball Valve Model (Hemobile)

The Hemobile consists of a cylinder actuated by a semi-rotating mechanism, generating a closed-loop, pulsatile flow without air in the circuit (Fig. 3b). The resulting semicircular motion produces low-shear, bidirectional flow patterns that resemble arterial pulsations more closely than continuous flow systems. However, specific data on shear rate or flow velocity are limited, making direct comparison to other models difficult (Table 2). Only one study, by van Oeveren et al. [20] (2012), has evaluated thrombus formation using this setup. While this restricts reproducibility assessment, the Hemobile may offer value in mimicking physiological waveforms and could merit further exploration in thrombosis research.

Roller Pump

The roller pump model (Fig. 3c) is designed to simulate blood flow under controlled conditions, offering potential improvements over the Chandler Loop [20]. It enables regulation of temperature (37°C), flow rate, circuit volume, and test duration. In some configurations, the system allows for intermittent or partial flow obstruction – so-called dynamic occlusion scenarios – to mimic conditions such as catheter pinching or flow stasis [20]. The roller pump is particularly suited for studying thrombus formation under controlled shear conditions and has been applied in intravascular catheter testing. However, like other in vitro macromodels, it lacks an endothelial surface, limiting its ability to replicate all aspects of in vivo thrombogenicity [21]. While promising, the roller pump has seen limited uptake, with only a few studies published to date [20, 21].

Badimon Chamber

The Badimon chamber is an ex vivo model for studying arterial damage and thrombosis, useful for assessing antithrombotic regimens [25–28]. It detects thrombus formation in native (non-anticoagulated) whole blood under flow conditions mimicking diseased coronary arteries (Fig. 3d). This apparatus uses a pump to draw blood from an antecubital vein via polyethylene tubing, passing it through a series of two or three cylindrical perfusion chambers replicating patent (212 s^{-1}) and mildly stenosed coronary arteries (1,690 s^{-1}), using porcine aorta strips as substrates [29]. Post-experiment, porcine strips with attached thrombi are removable for analysis. Thrombus formation occurs in about 5 min at a flow rate of 10 mL/min [30–32] (Table 2). This model evaluates antiplatelet medicines in the prevention of vascular disease and measures thrombus size via digital planimetry [29]. The Badimon Perfusion Chamber has been employed in exploring thrombogenic effects of diseases [33–35], pathological states [36], acute coronary syndromes [37–39], and pharmacological interventions [27, 28, 40, 41]. However, the Badimon chamber necessitates donor presence, hindering prolonged studies, and constraining experimental duration [29].

Shear-Induced Platelet Aggregation Model

The shear-induced platelet aggregation (SIPA) model, developed by Kim et al. [42], is a macrofluidic system designed to overcome the scale limitations of microfluidic assays (Fig. 3e). By operating under arterial shear conditions (~3,500 s^{-1}) (Table 2), it generates macroscopic thrombi – on the millimeter scale – representative of clinical thrombus sizes, which typically range from several hundred micrometers to centimeters, depending on vessel and pathology [42, 43]. The system consists of a closed-loop circuit with a roller pump that maintains constant pressure through a collagen-coated glass constriction. Lightly heparinized blood (~400 mL per

Fig. 3. Schematic overview of macroscopic arterial thrombosis models that involve flow. Rolling models (top row): **a** Chandler Loop: composed of silicone tubing formed into a loop, connected to a motorized pump to ensure continuous blood flow, immersed in a water bath. **b** Hemobile: features a ball valve design with macrofluidic channels without presence of air. **c** Roller pump: consists of a series of rotating rollers that compress flexible tubing, generating a controlled, pulsatile flow, in a water bath. Perfusion models (middle row): **d** Badimon chamber: includes an ex vivo arterial segment mounted within three flow chambers, with adjustable flow rates, draining blood directly from the patient. **e** SIPA model: closed-loop circuit with roller pump initiates clot formation in collagen-coated constriction, collagen-coated glass constriction with a 2.5 mm throat diameter resulting in SIPA clot. Diagnostic models (bottom row): **f** TEG: comprises a rotating cup and pin system that measures the viscoelastic properties of blood, providing detailed information on clot formation and stability. **g** ROTEM: features a rotating pin within a fixed cup, designed to assess clot elasticity and strength through rotational thromboelastometry. **h** GTT: incorporates a capillary tube system with two ceramic balls, an area characterized by high shear stress enabling platelet activation and aggregation, an area characterized by low-shear stress, enabling thrombin generation and fibrin formation and resulting in a thrombotic occlusion by the presence of thrombi. Created with BioRender.com.

Table 2. Specific applications of each macroscaled arterial thrombosis model

Model	Suitable for endpoint measurement
Chandler Loop	• Studying hemodynamics and device-blood interaction related thrombosis • Mimicking arterial shear rates
Modified Chandler Loop	• Testing interactions with stents, artificial heart valves, and catheters • Measuring plasma markers and clot weight • Studying the clot structure and mechanics
Hemobile	• Simulating physiological arterial pulsations • Studying thrombus formation with more physiological flow patterns
Roller Pump	• Investigating thrombus formation under controlled flow conditions • Testing intravascular catheter interactions
Badimon Chamber	• Assessing antithrombotic regimens • Studying artery damage and thrombosis • Evaluating thrombus size using digital planimetry
SIPA Model	• Generating macroscopic thrombi that is similar to thrombi in larger arteries, suitable for mechanical characterization, under arterial hemodynamic conditions • Studying shear rate and thrombus structure
TEG and ROTEM	• Real-time analysis of clot formation and disintegration • Diagnosing bleeding in high-risk patients
GTT	• Assessing thrombotic and bleeding status of patients • Evaluating thrombus stability and rate of thrombolysis • Testing without anticoagulants

experiment) is circulated to form white SIPA clots, which are mechanically stable and retrievable without structural damage for further analysis. Unlike geometrically variable systems such as the Chandler Loop, the SIPA model features a well-defined flow environment, allowing for accurate computational fluid dynamics simulations to characterize shear distribution and guide experimental interpretation. This enables refinement of the model and enhanced mechanistic insights into clot formation dynamics. Despite its advantages, the main limitation of the SIPA model remains the high volume of blood required, which can hinder repeatability and translational application in human studies.

Thromboelastography and Rotational Thromboelastometry

Thromboelastography (TEG), introduced by Hartert in 1948 [44] and its modern adaptation, rotational thromboelastometry (ROTEM) [45, 46], offer real-time assessment of clot formation and lysis in whole blood, reflecting viscoelastic properties at low-shear rates (~0.1 s^{-1}) (Table 2). TEG uses a rotating cup and a suspended pin, while ROTEM inverts this configuration, with a stationary cup and oscillating pin tracked by an optical system (Fig. 3f, g). Both tools are primarily applied in clinical settings for managing bleeding risk [47, 48] and are rarely employed in academic research. Their relevance to thrombus formation mechanisms remains limited due to their low-shear conditions and inability to replicate physiological flow, platelet adhesion, or vasculature [49].

Global Thrombosis Test

The Global Thrombosis Test (GTT, Thromboquest Ltd) is a point-of-care device that evaluates thrombus formation and endogenous fibrinolysis in non-anticoagulated blood [50, 51]. Unlike low-shear assays, GTT uses shear stress to activate platelets and form thrombi under conditions mimicking arterial flow rates (Table 2). Blood is introduced into a conical plastic tube containing a steel ball positioned near the upper end (Fig. 3h). A flat segment along the inner wall prevents full occlusion, allowing blood to pass through narrow gaps around the ball. This configuration generates localized high shear stress – ranging from ~100 s^{-1} to over 12,000 s^{-1} – particularly near the upper bearing, where platelet activation is triggered [52]. As thrombi form, they progressively obstruct the lower bearing, halting flow. Subsequent endogenous thrombolysis leads to restoration of flow, allowing for quantification of both

occlusion and lysis times [53, 54]. Two newer versions of the original GTT-1 device [52] are currently available: GTT-2 introduced automated data recording and improved reproducibility, while GTT-3 further includes thrombus stability metrics and real-time lysis kinetics [55–58]. As with the Badimon chamber, a key limitation of the GTT is that the test must be performed immediately on fresh blood, thus presence of the patient is required. However, its use of non-anticoagulated blood and ability to assess spontaneous thrombolysis make it particularly relevant for evaluating thrombotic risk (Table 3) [50].

Microfluidic Flow Models

Microfluidic flow models in thrombosis studies have gained prominence in recent years thanks to rapid developments in microfabrication technology [58]. In general, these are transparent flow models with channels that have micrometer dimensions. The microchannels can incorporate endothelial cells, extracellular matrix coatings, and other relevant components to study thrombosis under physiological flow conditions. While the fabrication steps may vary depending on the desired channel geometry, in general, a master mold is prepared by etching the desired pattern or channel onto a silicon wafer via lithography, then polydimethylsiloxane (PDMS) is poured over this mold and allowed to solidify by curing. The PDMS model is then peeled off from the master mold, and the channels are sealed via a glass coverslip which can be coated with desired prothrombotic materials. The PDMS model and the glass coverslip can be bonded irreversibly, often via plasma activation or reversibly, by vacuum bonding or a clamping device. Alternatively, models can be fabricated by other microfabrication methods such as micromilling or 3D printing from materials like PMMA or acrylic [59, 60]. To study thrombus formation, microfluidic models are partially or fully coated with a prothrombotic surface to initiate thrombus formation. The most common triggers used to initiate clotting are type I collagen, tissue factor, or a mix of both [61–65], while in other studies fibrinogen or von Willebrand factor coatings have been used to stimulate recalcified blood [66, 67].

A major advantage of these flow-based in vitro assays is that they allow a precise control over the shear rate to mimic arterial, venous, or pathological blood flow conditions [68]. Additionally, microfluidic models require only a small volume of blood and can therefore be patient- or disease-specific. As previously mentioned, arterial thrombosis is often associated with atherosclerotic plaques that lead to a stenosed vessel geometry. These complex geometries can be mimicked using microfabrication methods [69]. Additionally, being made of optically transparent materials, microfluidic models allow for real time imaging of thrombus formation via optical microscopy for a more comprehensive understanding of mechanisms and interactions involved in thrombus formation.

The simplest microfluidic models use straight channels (models in Table 4). Alternatively, a common geometrical feature of microfluidic models for arterial thrombosis research is a stenosis geometry to mimic the presence of atherosclerotic plaques (models in Table 5). Also common is the addition of a bifurcation as a pressure relief system to achieve a more physiologically relevant pressure range at especially high arterial shear rates (models in Table 6).

Surface Coatings and Cellularization

Since in vitro models are only reductions of a very complex physiological system, it is important to interpret the results with caution. An important aspect is the coagulation trigger. The majority of reported microfluidic in vitro models have used fibrillar type I and III collagen and/or tissue factor coating as coagulation trigger. Collagen I is an especially popular choice and is widely used in platelet studies since it triggers a strong thrombotic response [70]. However, different sources of collagen, often of nonhuman origin, have been used in different studies which may influence the effectiveness of platelet binding and the clinical translation. Also, the use of collagen as the procoagulant surface may overestimate the role of platelet-collagen binding compared to other platelet-vessel wall component interactions. Popular alternatives for procoagulant coatings are recalcified blood perfusion over fibrinogen, activated endothelial cells or a von Willebrand factor coating [66, 67]. Two interesting studies by Karel et al. [60] and Penz et al. [71] used atherosclerotic plaque material as a thrombogenic surface to initiate clotting. Karel et al. compared thrombus formation on atherosclerotic plaque material and type I collagen and found that plaque material was similarly effective as collagen in triggering clotting. However, blood from patients with hematological disorders treated with Bruton tyrosine kinase inhibitors showed reduced platelet deposition on atherosclerotic plaque materials whereas platelet deposition was not altered on collagen [70]. Karel et al. also characterized the atherosclerotic plaque material coating methods and their effectiveness in platelet adhesion [60]. They found that an oxygen plasma treatment of the glass surface prior to spin

Table 3. Overview of experimental conditions including flow rate and pros and cons of macrofluidic thrombosis models

Device	Shear rate	Additional parameters	Advantages	Disadvantages
Chandler Loop	400–600 s^{-1}	• Tube material: PVC • Inner diameter: 3–8 mm • RPM: 15–40 • Temperature: RT, 37°C • Blood: citrated (human, others) blood, plasma, platelet-free plasma, heparinized blood, pooled plasma • Coagulation activation: CaCl2, saline, thrombin • Clotting time: 15–120 min	• Thrombi structurally similar to patient thrombi • Simple • Cheap	• No standardized protocols • Limited range of shear rates • Presence of air in the tube • No real-time microscopic observations
Hemobile	14,500 s^{-1}	• Flow: 40 mL/min • Tube material: PVC • Inner diameter: 3 mm • Frequency: 60 beats/min • Temperature: 37°C	• No air in the tube • No compressive mechanical elements • Emulates pulsatile flow	• Only a few studies are available • No real-time microscopic observations
Roller pump	Not mentioned	• Velocity: 79±4 mm/s • RPM: 15 • Temperature: 37°C	• Ability to modify orientation of blood flow • No air in the tube	• Only a few studies are available • No real-time microscopic observations
Badimon chamber	212 and 1,690 s^{-1}	• Flow rate: 10 mL/min • Temperature: RT, 37°C • Duration: 5 min	• Replicates patent and mildly stenosed coronary arteries • Fast • Native blood is used, versatile in terms of thrombogenic coatings • Assessment of pro/anti-thrombotic effects on blood	• Immediate discard of blood • Presence of patient is mandatory • No real-time microscopic observations
SIPA	3,500 s^{-1}	• Glass tube: 12 mm inner diameter • Stenosis: 80%, 2.5 mm diameter • Coating: 100 mg/mL type 1 fibrillar collagen solution in 0.9% saline • Blood: heparinized (3.5 IU/mL) porcine blood • Coagulation activation: $CaCl_2$ • Volume: 400 mL • Flow rate: ~1 L/min • Pressure: 30 mm Hg (roller pump)	• Resemblance to clinical conditions in terms of flow rate and stenotic geometry • Controlled in vitro flow conditions • Retrievable clot without structural damage	• Large amount (400 mL) of blood required for testing
GTT	100–32,000 s^{-1}	• Blood: native blood • Temperature: 37°C	• Native blood is used • Clinical use (thrombotic status of patient through analysis of thrombolysis and thrombus stability) • Reproducibility • Automatization • Commercially available • Standardized protocol	• Presence of patient is mandatory • Expensive

Table 4. Overview of the characteristics of microfluidic models with straight channels, including methods of thrombus formation and the main research findings

Author, date	Device description	Shear rate	Coagulation trigger	Pump	Main findings
Brinkman et al. 2022 [92]	Transparent parallel-plate flow chamber sealed with a glass coverslip (width 3 mm, depth 50 μm, length 300 mm)	1,000 s^{-1}	Whole blood flown over coverslip coated with microspots containing Horm type I collagen and Tissue factor	Syringe pump	In DOAC-treated whole blood, the combination of PCC and FVC improved clotting time under static conditions, whereas under flow a complete correction of fibrin formation was observed. Simultaneous measurement of fibrin generation, platelet deposition, and platelet activation possible
Cadroy et al. 2000 [62]	Parallel-plate flow chamber	650 and 2,600 s^{-1}	Whole blood flown over coverslip coated with collagen type I or TF	Peristaltic pump	Possible to show that platelet thrombus formation was influenced by genetic variations in the GPIIIa platelet receptor. This effect depends on the blood flow rate and the nature of the thrombogenic stimulus
Cho et al. 2021 [67]	PDMS artery-mimicking multichannel interchangeable modular device with co-cultured HUVECs* and HASMCs*, circular channels	N/A	N/A	Peristaltic pump	A novel microfluidic model that can be modular and interchangeable depending on the desired experiment of thrombosis. Long-term cell culture is possible
Jain et al. 2016 [93]	6 independent microchannels (each 400 μm wide, 100 μm high, 2 cm long) on the PDMS block with the dimensions of a standard glass slide (75 × 25 mm) lined with endothelial cells	750 s^{-1}	Whole blood flow through the channel lined with endothelial cells that can be pretreated with TNF-alpha	Syringe pump	Thrombi formed in channels lined with endothelium resemble in vivo clots in shape and are different from thrombi formed on bare collagen surfaces, emphasizing the importance of incorporating the endothelium in these models
Karel et al. 2021 [70]	Transparent parallel-plate flow chamber sealed with a glass coverslip (width 3 mm, depth 50 μm, length 300 mm). Known as "Maastricht chamber"	1,500 s^{-1}	Whole blood flown over a homogenate of human atherosclerotic plaques that was coated on glass coverslips by conventional manual droplet coating or by spin coating	Syringe pump	The most homogeneous plaque coating and highest platelet adhesion was obtained upon plasma treatment followed by spin coating of the plaque material. Manual plaque coating on non-plasma treated coverslips yielded lowest coating homogeneity and platelet adhesion and activation

Table 4 (continued)

Author, date	Device description	Shear rate	Coagulation trigger	Pump	Main findings
Walton et al. 2017 [63]	PDMS chip with height, 51 μm; width, 500 μm	750 s^{-1}	Whole blood flown over patterned fibrillar collagen spots	Continuous microfluidic mixer	Higher hematocrit accelerated thrombus growth, exposing a direct, prothrombotic effect of increased hematocrit on thrombus formation
Yue et al. 2016 [65]	Bioflux plates coated with fibrillar collagen	1,500 s^{-1}	Whole blood flown over collagen-coated surface	Bioflux 200 system	Whole blood perfusion assay shows MINK1−/− platelets fail to form large thrombi over a collagen surface under arterial flow condition
Cosemans et al. 2005 [59]	Transparent parallel-plate flow chamber sealed with a glass coverslip (width 3 mm, depth 50 μm, length 300 mm). Known as "Maastricht chamber"	1,000 s^{-1}	Whole blood flown over collagen or atherosclerotic plaque material coated coverslip	Syringe pump	Possible to show that plaques rapidly triggered platelet adhesion and aggregation. The plaque homogenates were similarly active as native type I collagen fibers
Penz et al. 2005 [71]	Parallel-plate flow chamber with atheromatous plaque immobilized coverslips Model known as "Maastricht chamber"	1,500 s^{-1}	Whole blood flown over glass coverslip coated with atheromatous plaque material	Syringe pump	Results show platelet activation is the initial trigger leading to arterial thrombus formation as opposed to the common view of coagulation activation due to the TF present in plaques

DOAC, direct oral anticoagulants; FVC, factor V concentrate; PCC, prothrombin complex concentrate; HUVECs, human umbilical vein endothelial cells; HASMCs, human aortic smooth muscle cells; MINK1−/−, misshapen-like kinase 1.

coating of plaque homogenates yielded a more homogenous coating and higher levels of platelet adhesion as compared to manual droplet coating [60].

For accurate modeling of physiological conditions, ideally experiments should be performed at 37°C, but for practical reasons experiments are often conducted at room temperature. The earlier mentioned study of Karel et al. [60] found that on collagen surfaces, thrombi were larger and more contracted when formed at 37°C compared to room temperature, while on plaque surfaces the thrombus was not affected by temperature.

Cho et al. [67] designed a modular artery-mimicking flow model to study the inflammatory response of endothelial cells and the hemodynamic effects of stenosis. To mimic the structure of the arterial wall, they co-cultured endothelial and smooth muscle cells, with the endothelial cells aligned axially and the smooth muscle cells laterally inside circular channels. To mimic inflamed endothelial cell conditions, the cells were treated with TNF-alpha. This model is especially interesting for showing the versatility and the possible cell culture and design approaches for closely mimicking arterial vascular structures. Also, this model shows the modularity possible with microfluidic models. An additional mid-module that can be placed between two other parts was designed to be interchangeable to incorporate either straight or stenotic channel modules to observe the effects of stenosis, while additional modules like a mixer module and a concentration gradient generator module were also designed. The concentration gradient generator module allowed a different concentration of TNF-alpha to be administered in different channels to study the dose dependency of the cellular response [67].

A "thromboinflammation-on-a-chip" model by Qiu et al. [72] allows long-term culture of endothelial cells

Table 5. Overview of the characteristics of microfluidic models with a stenotic channel design, also including methods of thrombus formation and the main research findings

Author, date	Device description	Shear rate	Coagulation trigger	Pump	Main findings
Deng et al. 2022 [85]	PDMS chip with a stenosis region of a 50% reduction in channel size, the channel diameter was 650 μm and the stenotic region 300 μm	Inlet wall shear stress chosen as 20 dyne/cm^2, resulting in an estimated stenosis shear stress of 2,100 dyne/cm^2	ADP, collagen, TRAP-6, and U46619 were employed as agonists for platelet activation and flown through the chip	Peristaltic pump	Possible to show a significant enhancement in platelet aggregation when both stenosis and an agonist were present, thus suggesting a synergistic effect of atherogenic blood flow disturbance and circulating factors on platelet activation
Karel et al. 2022 [60]	Two parallel-plate perfusion chambers: a non-stenotic flow chamber (height 50 μm, width 3.0 mm, length 30 mm) and a stenotic flow chamber (height 50 μm, width 500 μm, length 30 mm). The stenotic region producing 60% occlusion. Both chambers consisted of a transparent polycarbonate block with a rectangular space, with or without stenosis	1,500 s^{-1}	Perfusion of whole blood over collagen type I or atherosclerotic plaque material	Syringe pump	Possible to identify an increase in shear rate up to 3,900 s^{-1}, due to 60% stenosis, decreasing platelet deposition and thrombus parameters on plaque material but not on collagen when compared to a laminar shear of 1,500 s^{-1}. Showed that treatment decreased platelet deposition around the stenosis
Nguyen et al. 2020 [94]	PDMS chips with circular microchannels from 100 μm to 500 μm with a concentric and eccentric geometries at 63% and 84% stenosis		Perfusion of whole blood over collagen type I coated channel	Syringe pump	A novel method for fabricating PDMS chips with circular cross-sections
Westein et al. 2013 [66]	PDMS, channel with varying % of stenosis	1,000 s^{-1} upstream and 5,000 s^{-1} at peak of stenosis (80%)	Perfusion of whole blood over vWF/fibrinogen coating in discrete patches	Syringe pump	Reported a Reynolds number of 1.2 (at 80% stenosis)
Lui et al. 2019 [74]	PDMS chip with either straight channels with uniform rectangular cross-section (600 μm wide, 200 μm high) or stenosed channels with straight regions (600 μm wide, 200 μm high) Each stenosis channel contained 4 consecutive stenoses of the same percentage area reduction (50%, 70%, or 90%), connected by regions of straight channel	1,800, 3,000, 6,600 s^{-1}	Perfusion of whole blood over bovine type I collagen coating	Syringe pump	Possible to identify differences in thrombus size between straight channels and stenosed channels from the same donors, and size differences between the 3 shear rates used among the same donors

Table 5 (continued)

Author, date	Device description	Shear rate	Coagulation trigger	Pump	Main findings
van Rooij et al. 2020 [95]	2 types of stenotic chambers: The stenotic section of the two devices differ in stenotic length (1,000 vs. 150 μm) and contraction angle of the stenosis (15° vs. 80°)	Shear rates higher than 3,000 s^{-1}	Perfusion of whole blood over collagen-coated surface	Hydrostatic pressure due to the elevated blood reservoir position	Possible to compare the influence of the stenotic region length on thrombus properties
Li et al. 2014 [76]	PDMS chip with stenosis designed and validated to simultaneously address initial shear rates of 500, 1,500, 4,000, and 10,000 s^{-1} within each of the four identical stenoses, with varying shear rates	Varying shear rates at the same time in different channels, all higher than 500 s^{-1}	Perfusion of whole blood over fibrillar equine collagen-coated surface	Gravity-induced pressure in syringes. The pressure was held constant by optically sensing fluid height and controlling syringe position by a linear actuator	Possible to identify occlusion time with varying shear. Thrombi formed within the stenosis region showed high concentrations of platelets with low concentrations of fibrin at high shear rates and red blood cell-rich thrombi at low-shear rates
Costa et al. 2017 [73]	PDMS cast in 3D-printed molds using patient data of stenotic vessel	1,000 s^{-1} inlet shear rate	Recitrated blood flown through stenotic channel lined with HUVECs	Syringe pump	A novel method for fabricating PDMS chips from patient vascular data with accurate geometry
Akhter et al. 2022 [77]	A PDMS chip with a main channel and a supporting channel with varying stenosis rates and functioning as a local junction region where collagen is exposed to the main channel via a porous region (200 μm × 50 μm)	Inlet shear rates of 2000 and 3,000 s^{-1} to achieve the shear rate of ≈1,890 s^{-1} (peak of 45% stenosis) and 3,450 s^{-1} (64%)	Whole blood exposed to collagen perfused through porous stenotic region	Syringe pump	A unique design allowing local delivery of atherosclerosis-mimicking material coupled with different rates of stenosis
Gao et al. 2024 [78]	A PDMS chip of multiple channels with different number of stenotic segments (80%) resulting in different shear gradient times in different channels	Input shear rate of 1,000 s^{-1}, leading to peak shear rate at the stenosis of 5,200 s^{-1}	Whole blood exposed to fibrinogen coated surface	Syringe pump	Possible to study the effect of multiple stenoses or shear gradient on platelet activation/attachment on fibrinogen surface
Watson et al. 2024 [79]	A PDMS chip with a sudden expansion geometry (a 200 × 50 μm channel opening to a channel of 400 × 50 μm)	1,000 s^{-1}, 5,000 s^{-1}, 10,000 s^{-1}	Whole blood exposed to collagen-coated surface	Syringe pump	Possible to study effects of circulatory support devices and stenosis

and monitoring of thromboinflammation by stimulation of these cells via TNF-alpha. This model supports the long-term culture of endothelial cells under flow for several weeks through its hydrogel-embedded channels. Using this model, Qiu et al. mapped out the phases of clot resolution in thromboinflammation and investigated the mechanism of potential therapeutic agents in preventing or resolving microvascular thrombosis [72].

Stenotic Geometries

Atherosclerotic plaques cause a stenosis in the vasculature. Several studies utilized microfluidic devices to study the impact of a stenotic geometry on arterial thrombosis [66, 73, 74]. Lui et al. [74], for instance, compared thrombus formation in channels designed with consecutive stenotic regions that increase in stenosis percentage (% cross-sectional area reduction) and showed that the thrombus size increased with increasing stenosis percentage and with the initial shear rate (Fig. 4a). Additionally, they modeled shear rate at peak stenosis and found a profound increase in the shear rate with increasing stenosis percentage. This dramatic increase of shear rate in peak stenosis region was reported in other studies modeling stenotic geometries as well [66, 73–75]. Also, Westein et al. [66] developed a microfluidic model with varying stenosis percentages (Fig. 4b). They chose a fibrinogen and von Willebrand Factor coating to represent the surface of a growing thrombus and saw that the combination of the shear forces due to the stenosis and weakly platelet-activating von Willebrand factor/fibrinogen surface was sufficient to observe thrombus formation downstream of stenosis [66]. They found that platelet aggregation post-stenosis was dependent of the stenosis percentage. Furthermore, they found that the microfluidic model peak mean wall shear rate (5,000 s^{-1}) was similar to the rates in a human carotid artery (3,692 s^{-1}) but the Reynolds number at the stenosis was lower (Re = 1.2) in the microfluidic model compared to the human carotid (Re = 4,300), due to the smaller dimensions of the model [66].

A high-throughput model by Li et al. [76] employs 4 parallel channels with identical stenoses but varying initial shear rates (500 s^{-1}, 1,500 s^{-1}, 4,000 s^{-1}, and 10,000 s^{-1}) to study shear rate influence on thrombus formation in a single experiment (Fig. 4c). Additionally, they studied the efficacy of acetyl-salicylic acid (ASA) at different shear rates. Their findings demonstrate that ASA, even at doses 20-fold higher than standard, failed to prevent occlusion at high shear rates (>4,000 s^{-1}) while at lower shear rates (500 and 1,500 s^{-1}), it significantly delayed occlusion and reduced thrombus formation [76].

An atherothrombosis model by Akther et al. [77] was designed to locally expose flowing blood to plaque components at the region of a stenosis via a porous hydrogel membrane in order to more closely mimic in vivo plaques, where plaque components are exposed at the site of the stenosis (Fig. 4d). The model consists of a main and a supporting channel, connected at the stenosis point via a membrane. Whole blood flows through the main channel while plaque components flow through the supporting channel Akther et al. [77] reported increased platelet accumulation with increased stenosis percentage and shear rates. They also validated their model as a drug testing platform by testing the antiplatelet efficacy of a known drug, aspirin, and showed that, in therapeutic doses, aspirin prevented or delayed platelet adhesion in their model [77].

The majority of microfluidic models until now were produced using photo-lithography and soft-lithography techniques. These techniques offer high microfabrication precision but come with challenges like costs and requirement of cleanroom facilities and limitations in producing some 3D geometrical features [69]. To overcome these limitations, some groups have opted for alternative and cheaper fabrication techniques such as 3D-printed models. A key advantage of 3D printing compared to photolithography is that more complex geometries can be fabricated, and vessels can be made circular instead of rectangular, better mimicking arteries. For instance, Costa et al. [73] recently demonstrated a patient-specific stenosed vessel model where they 3D printed a scaled down model of the vessel geometry based on computed tomography angiography (CTA) data (Fig. 4e). Computational fluid dynamics analysis comparing the CTA and the scaled down flow model revealed that the 3D-printed model achieved comparable increases of shear rates at stenosis (>10,000 s^{-1}) [73]. The model also showed similar recirculation zones post stenosis as the original CTA, though in a smaller region. The difference of the flow patterns and recirculation zones between the CTA and the flow model was attributed to the significantly higher Reynolds numbers in the larger model compared to the flow model. Upon endothelization, thrombus formation was observed only in the stenotic models as opposed to the straight one and localized at or downstream of the stenosis, emphasizing the role of altered flow in thrombus formation [73]. 3D-printed microfluidic models can thus accurately capture vessel geometries based on patient vasculature, to improve our understanding of the role of vessel geometry in thrombosis.

Gao et al. [78] employed a microfluidic model to simulate the transient shear stress conditions characteristic of arterial stenosis, revealing that the rise and fall phases of shear significantly enhance platelet activation and aggregation via a von Willebrand factor-dependent mechanism (Fig. 4f). Blood samples were exposed to a maximum shear rate of 5,200 s^{-1} for 68.8 milliseconds with an initial shear rate of 1,000 s^{-1}, simulating the rapid

Table 6. Overview of the characteristics of microfluidic models with pressure relief and branching channel design, also including methods of thrombus formation and main research findings

Author, date	Device description	Shear rate	Coagulation trigger	Pump	Main findings
Berry et al. [61] (2021)	PDMS bifurcating pressure relief flow chamber with width: 500 μm, height: 70 μm	1,000 s^{-1}	Collagen – tissue factor patch	Syringe pump	Possible to generate occlusive thrombi and measure "time to occlude" using pressure relief mode
Colace et al. [75] (2012)	PDMS chip with 8 parallel channels width: 250 μm, height: 60 μm, sealed with a glass coverslip. The parallel channels can be used as pressure relief coating every other channel surface	Inlet shear rate 1,000 s^{-1} under constant flow rate or pressure relief mode. At 80% of full channel occlusion, shear rates reached a maximum value of ≈7,000 s^{-1}	Blood perfusion over lipidated TF and fibrillar collagen type I surface	Syringe pump	Possible to compare pressure relief and constant flow methods and show difference of thrombus growth resistance under the two different pressure conditions
Muthard et al. [81] (2012)	PDMS device with a channel of 250 μm wide and 60 μm high with an opening to a micropost collagen scaffold region (50 μm × 60 μm) with pressure control ports	1,130 s^{-1}	Blood perfusion over collagen/TF or collagen type I scaffold region	Syringe pump	The collagen scaffold region functions as a side view imaging site of thrombus growth, contraction, and permeation. The device further allows for investigating thrombus permeation in the presence of a controlled pressure drop
Tsai et al. [96] (2012)	PDMS microfluidic networks of branching microchannels with the smallest channels at 30 μm in width and height	High shear rate regime defined as 10–40 dynes/cm^2	Whole blood perfused over STX2-exposed endothelial cells	Syringe pump	Possible to expose flowing blood to various channel sizes and shear rates simultaneously
Qiu et al. [72] (2025)	A hydrogel-based microfluidic model with channels that bifurcate Channel cross-section 20 × 20 μm	–	Whole blood perfused over endothelial cells stimulated with TNF	Syringe pump	Possible to study thromboinflammation in microvascular thrombosis. Long-term culture of endothelial cells and mapping out phases of clot resolution
Belenkovich et al. [97] (2024)	A PDMS microfluidic model with a network of branching channels inspired by the cerebral vascular system The successive channel diameters of the branches were calculated according to Murray's law	300 s^{-1} and 1,000 s^{-1}	Whole blood perfused over type I collagen coated surface	Syringe pump	The branched network of channels shows thrombi formation favoring bifurcation zones compared to straight channels

STX2, Shiga Toxin 2.

acceleration and deceleration of blood flow through narrowed arterial segments [78]. They also assessed the effects of antiplatelet agents such as ASA, ticagrelor, and tirofiban on shear-induced platelet activation. This model highlights the importance of considering transient shear dynamics in the development of antithrombotic therapies and the design of in vitro models for arterial thrombosis research.

A recent study by Watson et al. [79] introduced a microfluidic model incorporating a sudden expansion geometry to investigate SIPA under nonphysiological flow conditions, simulating environments such as those found in mechanical circulatory support devices. The model enables variation of shear rates (1,000–10,000 s^{-1}) by a backward facing step geometry. Such geometries are used for modeling circulatory devices or outlets of stenotic regions [66, 79]. Notably, the study demonstrated that increased hematocrit (with the level being varied from 0 to 60%) enhances platelet margination and adhesion, while blockade of integrin $\alpha_{IIb}\beta_{III}$ significantly reduced both platelet accumulation and aggregate size [79].

Pressure Relief Channels for Physiological Pressure Ranges

In microfluidic studies, the most common method for perfusion is the use of constant flow rate via a syringe pump. However, models which use constant pressure flow pumps instead or models that include a bypass channel to allow for continuous blood flow during thrombus growth can be more physiologically relevant [61, 68, 80]. At high-flow rates, the high-pressure buildup poses an additional technical challenge since the clot is easily flushed away. Berry et al. [61] proposed a bifurcated flow model to overcome this unphysiologically high-pressure buildup while using a syringe pump with constant flow. One arm of the branching channel was coated with a collagen and tissue factor patch while the other arm acts as a bypass channel allowing blood to flow while an occlusive thrombus grows [61]. Additionally, they designed two extra inlets for introducing EDTA to stop clotting after the procoagulant patch to localize the "injury site" and prevent thrombus growth downstream. Downstream of the EDTA inlets a herringbone-patterned surface functions as an on-chip chaotic mixer (Fig. 4g). They suggest that, by eliminating downstream thrombus formation, this model allows for a more accurate method to measure the time for the thrombus to occlude. Colace et al. [75] used a similar flow model with 8 channels that can be used both as constant flow and pressure relief model depending on the setup (Fig. 4h). The 8 channels are connected to a single outlet and 8 inlets. In the constant flow setting, all 8 channels are used for thrombus formation while in the pressure relief mode, only 4 channels are coated with a thrombogenic trigger, and the neighboring 4 channels are left as bypasses for blood flow. By comparing the two modes using the same model and clotting trigger (TF and collagen), they observed that the pressure relief mode yields thrombi which can withstand higher shear rates before embolization as compared to the constant flow mode [75].

Another model with an adjustable pressure gradient was designed by Muthard et al. [81]. This model allows independent control over both the shear rate and the pressure gradients at arterial flows. Briefly, the model has a main channel with a single inlet and two outlets and three pressure ports (Fig. 4i). This model was used to evaluate the influence of pressure gradients on thrombus structure [81]. An additional feature was to create a scaffold region with collagen posts where the thrombus forms, providing a side-view window allowing observation of thrombus growth, contraction, and permeability by optical microscopy [81].

Discussion

In this review, we systematically evaluate current in vitro and ex vivo models of arterial thrombosis across macro- and micro-scales. Although such platforms are versatile, accessible, and amenable to replication, they are simplified representations of thrombosis and cannot fully capture the in vivo complexity. Because clinical relevance depends on how closely a model reproduces physiological conditions, we compare their strengths and limitations with an emphasis on physiological fidelity and translational applicability.

Macro-Scale Models

We examined a range of in vitro and ex vivo macrofluidic models developed to study thrombus formation under dynamic flow conditions. These systems – such as loop circuits and flow chambers – are widely used due to their relatively simple setup and longstanding application in thrombosis research. Compared to microfluidic devices, their larger scale enables modeling of hemodynamics in large vessels and macroscopic sized (millimeters) thrombi similar to patient thrombi in size. They allow studies on thrombus formation due to blood-material interactions and device-associated thrombogenicity. Another important advantage of macrofluidic systems is their capacity to simulate complex flow regimes, including turbulence and pulsatility, which are difficult to achieve in laminar microfluidic setups. However, the large scale of macrofluidic systems also introduces practical constraints, particularly regarding blood availability, donor variability, and the standardization of flow parameters across laboratories. Many models, such as the Chandler Loop, have been widely adopted despite recognized limitations in reproducibility and shear control [31]. Recent systems like the Hemobile and the SIPA model aim to improve flow regulation, particularly in replicating arterial shear gradients. The SIPA model offers a hybrid approach by generating macroscopic thrombi while maintaining

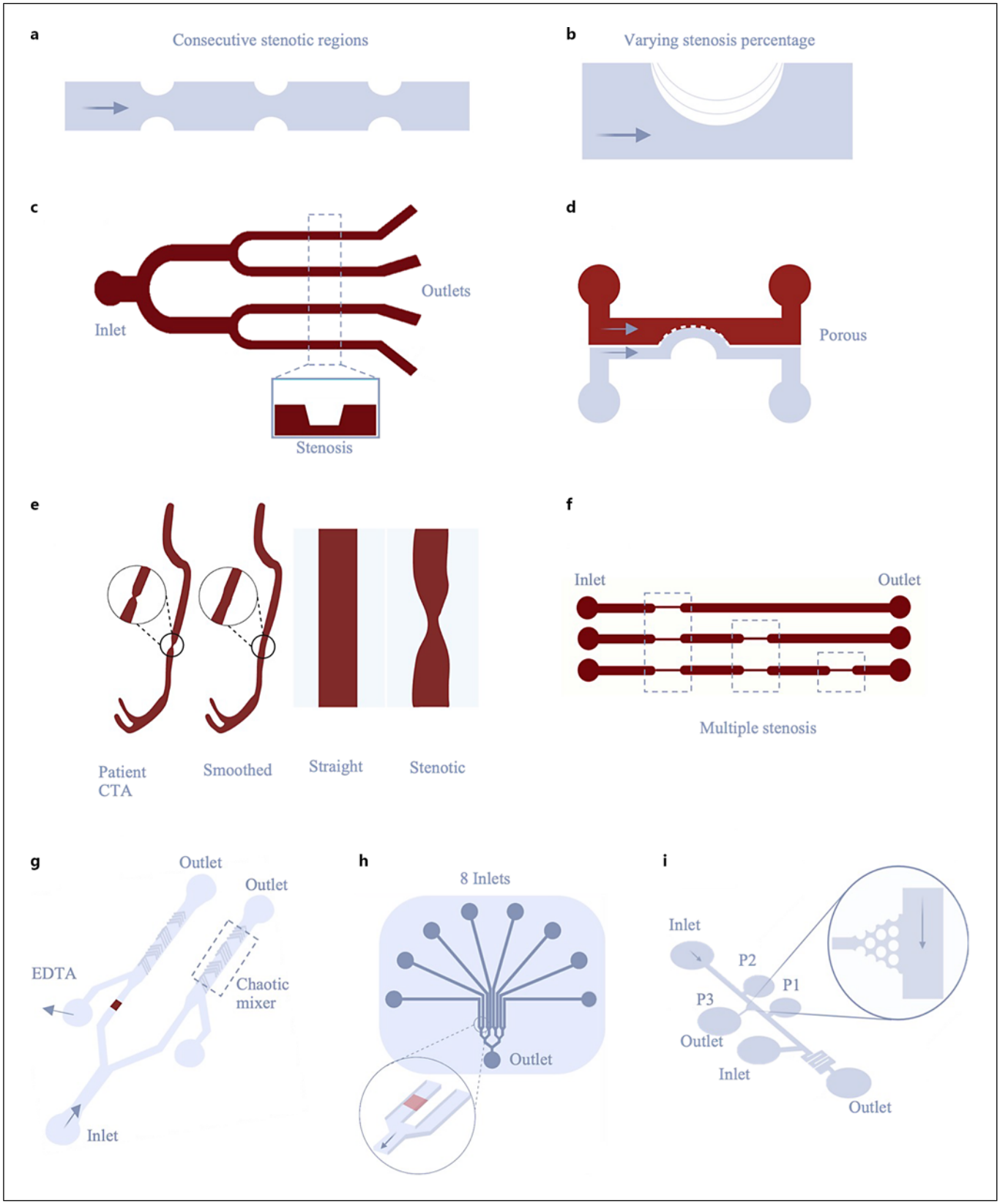

4

(For legend see next page.)

hemodynamic precision through a defined geometry, bridging the gap between micro- and macrofluidic platforms. The Badimon chamber, an ex vivo system, allows for thrombus formation using fresh patient blood and replicates the geometry of stenosed coronary arteries. Its ability to recreate near-physiological conditions makes it a valuable model, while the requirement of patient presence limits its widespread use.

While TEG and ROTEM are primarily clinical diagnostic tools for assessing coagulopathy, their inclusion here highlights the range of available systems for producing thrombi under a dynamic condition, despite their limited relevance for modeling arterial thrombosis. Lastly, the GTT stands out for combining physiological shear conditions with simplicity and automation. By using native, non-anticoagulated blood and detecting thrombus formation and lysis, it offers a clinically relevant, pharmacodynamically informative platform. However, its requirement for real-time patient sampling and its high cost may limit broader application [53, 56, 82].

In summary, macrofluidic models provide physiologically relevant tools for studying thrombotic mechanisms, particularly under high-flow arterial conditions. Their ability to model complex flow and incorporate large blood volumes makes them particularly suitable for evaluating thrombogenicity and device interactions. Nonetheless, limitations related to blood availability, reproducibility, and standardization persist.

Microfluidic Models

Microfluidic models have several advantages over macrofluidic models, most notably the precise control over shear rates and geometries, the requirement of smaller blood volumes and the opportunity to perform real-time high-resolution imaging of thrombus formation.

While their smaller scale mean experiments can be conducted with a smaller volume of blood, a limitation to consider for microfluidic models is geometric scaling. Scaling down thrombotic processes to fit within microfluidic devices can lead to challenges in replicating physiologically relevant flow conditions, particularly when attempting to reproduce high Reynolds numbers seen in larger vessels [68, 83]. While it is possible to reach arterial flow rates, the flow pattern, whether there is laminar, disturbed, or turbulent flow, is another matter and dependent on scale. Microfluidic models often do not exactly replicate the complexities of blood flow, which can significantly impact thrombus formation. In particular, limitations regarding mimicking pulsatile, disturbed, or turbulent flow make it challenging to study the influence of

Fig. 4. An overview of channel design features identified in arterial thrombosis microfluidic models. **a–f** Microfluidic models designed to study the influence of a stenotic geometry. **a** Model by Lui et al. [74] incorporating four consecutive stenotic regions with increasing stenosis percentage and therefore exposing the flowing blood to a pulsating shear rate. The peak stenosis shear rates are presented for each stenotic region for the same inlet shear. A significant increase in the shear rate is observed at stenosis. **b** Model with different percentage of stenosis by Westein et al. [66]. **e** Costa et al. [73] used CTA data of a patient with a stenosed vessel to 3D print a microfluidic model with accurate geometry. Whole blood is flown through the endothelialized channels of the models with and without the stenosis and thrombus formation is observed only in the stenotic model. **d** Atherothrombosis model by Akther et al. [77] showing the main channel for blood flow and the supporting channel for flowing plaque components, with the porous junction region connecting the two. The stenosis rate can be varied by changing the curvature of the stenotic region of the supporting channel. **c** This high-throughput model by Li et al. [76] employs 4 channels running simultaneously with varying shear rates (500, 1,500, 4,000, and 10,000 s^{-1}, allowing investigation of varying shear rates in a single experiment. The occlusion time and thrombus detachment were measured by monitoring the decrease in flow rate or its resumption after thrombus detachment. This model was also used to study the effect of several antiplatelet therapy doses and shear rates on occlusion time. **f** Schematic representation of microfluidic devices with multiple stenotic regions. One such multiple stenotic model (80% channel stenosis) by Gao et al. [78] was developed to study shear dependent platelet aggregation at atherosclerotic arteries. The shear gradient through the channel was varied by the number of stenotic regions and by the length of channels between stenoses. Platelet activation increased with increasing number of shear rise and fall (number of stenosis). Another multiple stenosis model mimicking a clinically severe stenosis percentage (85%) was developed by Flores Marcial et al. [91]. They perfused blood at a shear rate of 12,000 s^{-1}. In all stenosis cases (single, double and triple stenosis channels), the occlusive thrombus was formed in the first stenosis, leading to decreased blood flow to second and third stenoses. Microfluidic models with pressure relief channels in order to achieve physiological pressure ranges. **g** The microfluidic model by Berry et al. [61] uses a branched geometry with a single inlet and two outlets, allowing an occlusive clot formation at high shear rates in one arm while the other arm acts as a bypass for pressure relief. The additional post-thrombus EDTA inlets stop clotting downstream of the collagen and tissue factor patch, confining the thrombus growth to the injury site. **h** The 8-channel model used by Colace et al. [75] is conceptually similar, but offers higher throughput as each of the 8 channels can be used for thrombus formation in constant flow mode or 4 channels can be used for thrombus formation in pressure relief mode. **i** "Side-view" microfluidic model by Muthard et al. [81] with a main channel with 3 pressure ports for monitoring pressure and a region with collagen posts as the area for thrombus formation. This side-view design allows for in situ observation of thrombus growth and the separate pressure ports allow control of the pressure gradient independent of the flow rate through the main channel.

complex flow patterns observed in larger arteries with stenosis or in the presence of medical circulation devices. Therefore, extrapolating findings from microfluidic models to larger vessel conditions relevant to for instance thrombectomy studies may not be straightforward [66, 83]. There are prospects, however, for replicating more complex flow conditions in microfluidic devices. For instance, while not as common as constant flow syringe pumps, some studies employed a peristaltic pump to mimic arterial blood flow more closely [67, 84, 85].

Additionally, due to limitations of the fabrication methods, often simplified geometries with rectangular channels are used. This is not an accurate representation of a circular vessel and may lead to flow disturbances near the corners of the channel cross-section. However, there are alternative fabrication methods available for achieving circular geometries like 3D printing. Moreover, cellularizing the channel lumen often corrects for the rectangular channel design [69, 73]. Another method for achieving circular channels in PDMS models is to pour uncured PDMS through the initially rectangular channels and flow pressurized air through the channels, to allow the PDMS to evenly coat the channel lumen and cure it as a circular lumen [85].

Another limitation of microfluidic models is that, due to their small scale, they may favor platelet-surface adhesion over platelet – platelet accumulation, whereas occlusive arterial thrombi in vivo are often composed of accumulated platelets due to the high volume-to-surface area ratio of the artery. However, this limitation can be addressed by appropriate design of the channel geometry. An interesting study by Casa et al. [86] showed that in order to favor platelet – platelet adhesion, rectangular channels with a higher aspect ratio should be chosen, whereas for circular channels smaller diameters (<20 mm) yield the platelet – surface adhesion dominated.

A major consideration regarding microfluidic models is standardization. This review revealed an abundance of unique and interesting in-house designed flow models. While the flexibility to design models for specific research questions is an advantage of microfluidic technology, this feature makes it difficult to compare and relate findings from different studies. Additionally, it remains a challenge to judge the physiological relevance of each model. To improve the reproducibility and clinical value of findings obtained using microfluidic models, protocols and reporting of variables and findings should ideally be standardized. Griffin et al. [87] investigated the influence of several experimental design variables over the thrombus occlusion time. They found that collagen surface coating and channel fabrication method influenced the occlusion time, while the method of anticoagulation did not impact it. Fabrication methods which yielded more reproducible channels, therefore, the most consistent shear rates, also produced the most consistent occlusion times [87]. Additionally, fibrillar type I collagen led to more consistent occlusion times, which was attributed to the more stable interaction with von Willebrand factor compared to its interaction with nonfibrillar thin films of collagen [87].

A first set of key variables important for standardization are for the biochemical conditions: prothrombotic coating material and its source and concentration, the type of blood anticoagulant, and recalcification methods. An experimental parameter relevant to clotting that is important and not always reported is the experimentation temperature, which should ideally be body temperature but is often room temperature [88]. A second set of key variables concerns the dimensions of the flow model. Key parameters for mimicking physiological conditions are the absolute dimensions (vasculature size and geometry) as well as the ratios of various characteristic dimensions. Relevant ratios are for instance the height-to-width ratio of a channel, which influences whether platelet-platelet or platelet-surface interactions will dominate while the size of the thrombogenic trigger directly influences the thrombus size. Other important size ratios are the ratio of channel height to injury length, and the height of the channel in relation to the red blood cell size since this influences the viscosity of the blood [89]. A detailed table of the dimensional and dynamic parameters to consider in flow model design is presented in McCarty et al. [89]. A third set of key variables to consider are parameters describing the characteristics of flow that is generated in the model and how well these represent physiological flow. An important dynamic parameter describing the type of flow inside a channel is the Reynolds (Re) number that describes whether the flow is laminar or turbulent (Table 1). The inertial forces dominate over the viscous forces at high Re numbers, which is observed in stenosed vessels and bifurcations or valves. Such complex flow patterns are important features, especially in larger arteries; however, this is difficult to recapitulate in microfluidic models due to their smaller size where laminar flow dominates. Other dimensionless dynamic parameters like the Peclet and Dahmkohler numbers govern the rate of transport of molecules to the injury site by convection vs. diffusion and determine whether the rate of a reaction is transport-limited or reaction-limited, respectively (Table 1). Thrombus growth and structure will differ based on the characteristics of the flow inside the channel, making such parameters critical in choosing a model and comparing results amongst different studies. While shear rate is almost

Minimum Reporting Checklist for All Flow Based Arterial Thrombosis Models

Researchers should report, at a minimum:

1. **Model type and scale** — macro, microfluidic, or hybrid; commercial vs. custom-built.
2. **Geometry** — dimensions, lumen shape, presence and percentage of stenosis, bifurcation angles.
3. **Flow parameters** — method of flow generation (e.g., syringe pump, peristaltic pump, rotation), target shear rates or stresses, and how these were calculated.
4. **Reynolds number** *(and, where relevant, Peclet and Damköhler numbers)* to characterize flow regime.
5. **Blood source and handling** — species, anticoagulation type and concentration, storage time, temperature control.
6. **Thrombogenic surface or trigger** — coating material, cellularization, plaque homogenates, or biochemical triggers (e.g., TF, collagen).
7. **Experimental duration & temperature** — total perfusion time, any preconditioning steps, and time to endpoints such as occlusion or clot retrieval.
8. **Readouts and analysis** — imaging modality, resolution, biochemical/morphological endpoints, mechanical testing, and lysis protocols if applicable.
9. **Replicates and variability** — number of replicates, inter-assay and intra-assay variation.

Fig. 5. Summary box detailing a minimum reporting checklist for all flow-based arterial thrombosis models.

always reported in flow models, these other essential parameters, are seldom reported even though they influence the experimental conditions under the same shear rate and therefore the outcomes [89]. Finally, a fourth key point for standardization is in the analysis of read-out parameters to quantify thrombus structure from microscopy imaging, especially in image quantification where manual vs. automized analysis tools may vary in Results [88].

A comparative summary of all models, including physiological fidelity and reproducibility potential, is provided in online supplementary Tables 1 and 2. These tables also highlight patterns in model design and performance that inform both translational potential and the feasibility of standardization, which are further discussed below.

Reproducibility and Standardization

As summarized in online supplementary Table 1 (model appraisal) and online supplementary Table 2 (quantitative parameters), inter-lab differences often arise from methodological variation in the models themselves – particularly for microfluidics (channel dimensions, shear rate control, coatings/surface chemistry, pump type, sample handling) Macro platforms (e.g., Chandler loop) also vary in tubing diameter, anticoagulation, and thrombogenic surfaces, which can shift thrombus morphology/kinetics. Multicenter validation studies remain rare. A notable counterexample is the GTT, which benefits from a standardized commercial design and multicenter use. To enable comparability and future meta-analysis, we recommend adhering to the Minimum Reporting Checklist in Summary Box (Fig. 5), at a minimum, reporting device geometry, shear rate, Reynolds number (and, where relevant, Peclet/Damköhler numbers), thrombogenic surface/coating protocol, blood source and anticoagulant type/concentration, temperature and assay duration/endpoints, and replicates/variability.

Possible Pathways to Clinical Translation

Several models already illustrate translational potential: the Badimon chamber has been used with patient blood to assess antiplatelet effects under flow; the GTT is deployed clinically for thrombotic status; macro loops (e.g., Chandler-type) are used to screen device coatings. Parallel-plate chambers, while less anatomically complex than some microfluidic platforms, offer reproducibility that could lend itself to fixed-geometry, cartridge-style formats. In contrast, high-fidelity models such as SIPA or patient-specific 3D-printed vessels face challenges due to large blood volume demands or fabrication complexity. Microfluidic systems excel in shear control and low sample volumes, but their reliance on custom fabrication and high-resolution microscopy techniques impedes widespread standardization. Online supplementary Tables 1–2 suggest that platforms closer to translational evaluation tend to share practical features, low sample volumes, minutes-scale readouts, relatively simple/laminar shear profiles, and compatibility with automation. A possible pathway to clinical translation and diagnostics could involve: (1) converging on standardized geometries/coatings and shear calibration for a small set of reference platforms; (2) integrating rapid, operator-light readouts (optical, impedance, or flow-cessation) into closed cartridges; (3) conducting multicenter evaluations against clinical endpoints; and (4) where justified, layering in higher fidelity elements (patient-specific geometries, endothelialization) once manufacturing methods are established.

Table 7. Comparison of macromodels vs. micromodels based on their performance in mimicking in vivo conditions, requirements of blood volume, ease of use, customizability, and the suitable endpoint measurements as a brief guide

In vitro model parameters	Macromodels	Micromodels
Mimicking in vivo flow patterns and shear rates	Possible to achieve turbulent or disturbed flow to mimic flow patterns in stenotic, bifurcated, or pathological larger arteries	Laminar flow only, due to small scale. Ideal for flow patterns in smaller and microvasculature
	Difficult to fully characterize the shear rate inside tubular models due to turbulence (Chandler Loop, Roller pump, etc.)	Possible to achieve and characterize shear rates of physiological ranges
	In vivo flow patterns not mimicked in TEG, ROTEM, GTT	
Mimicking in vivo geometry	Tube diameter may be of similar diameters to larger arteries but always used in a loop form	Patient geometry can be mimicked in smaller scale (e.g., 3D-printed model from Costa et al.)
	Not mimicking vascular geometry in TEG, ROTEM, GTT	Possible to mimic microvasculature to scale
	Possible to design custom geometry macro-models (e.g., SIPA models mimicking stenosis)	Although less common, circular channels are possible in microfluidic models
		Stenosis of various percentage can be mimicked in smaller scale
Mimicking in vivo cellularization	Not possible in macromodels due to their large scale	Possible to line the channels with endothelial cells, smooth muscle cells, ECM components or atherosclerotic plaque material
		The modular model by Cho et al. [68]. concentrically lines their channels with both endothelial and smooth muscle cells to mimic the layers of arteries
Required blood volume	Often >1 mL of blood for tubular models	Often < 1 mL of blood for micromodels
	Especially larger volumes of blood required in SIPA model (4–5 mL)	
Customizability of design	Possible to adjust tube diameter and RPM or flow rate in tubular models	Possible to design complex channel geometries in smaller scales. Models can be designed and tailored specifically for studies in terms of geometry (channel dimensions, stenosis, bifurcation, or mimicking patient geometry), thrombogenic coating material, cellularization, and flow rates
	Possible to design custom macro-models (e.g., SIPA models mimicking stenosis)	
	Customization not possible for TEG, ROTEM, or GTT	The modular model by Cho et al. [68]. reveals the versatility and flexibility of micromodels
Ease of use/Requirements of specialty equipment	Macromodels are easier to use and commercial setups with standard protocols are available, especially for TEG, ROTEM and GTT, due to their diagnostic use	Micromodels can require a steeper learning curve for use and set up
		Although fabricating PDMS chip can be cheap and fast, the costs and effort of the design of custom models and investment in mold fabrication methods (photolithography, 3D printing) should be considered
Suitable/common endpoint measurements		
Real-time imaging during clot formation	Possible to monitor clot growth and clot formation time on a macroscale via camera in some tubular models	Possible to monitor clot formation and growth real-time via microscopy and at (sub)cellular resolution imaging of the clot components individually (fibrin, platelets, RBCs, vWF. . .) using fluorescence labelling
	Not possible to monitor real-time clot formation or growth at high resolution	

Table 7 (continued)

In vitro model parameters	Macromodels	Micromodels
Higher resolution imaging post-clot formation	Possible to study clot structure via various techniques (SEM, histology. . .) for clots made in tubular models	Possible to study clot structure via various techniques (SEM, histology. . .)
	Was possible to image clot components like fibrin, platelets and vWF for the SIPA clot	Possibly more difficult to handle and process small-scaled clots
	Not possible/performed on TEG, ROTEM, or GTT clots	
Mechanical characterization	Due to their relatively larger size, it is possible to test bulk mechanical properties of clots produced in tubular models via compression testing or local mechanical properties via nanoindentation	Due to their relatively smaller size smaller scaled mechanical tests like nanoindentation or AFM are more suitable for clots produced in micromodels
	TEG and ROTEM test the viscoelastic properties of blood clots	Possibly more difficult to handle and process small-scaled clots
Clot lysis tests	Possible to perform thrombus lysis experiments and measure lysis time in macromodels	Possible to perform and image lysis experiments in real time in micromodels

The choice of in vitro model depends on the specific research objectives, the aspects of arterial thrombosis being studied, and the available resources. Table 7 compares the macro- and microfluidic models based on their performance in mimicking in vivo conditions, required amount of blood, ease of use, and the suitable endpoint measurements as a brief guide. Overall, macroscale models like the Chandler Loop may capture complex or turbulent flow patterns, which may be relevant in thrombus behavior in mechanical thrombectomy studies. Conversely, microfluidic models can maintain functional endothelial layers and study endothelial cell-related aspects of thrombosis effectively, while this is not often seen in macromodels. Also, microfluidic models, unlike macrofluidic models, are compatible with real-time high-resolution microscopy imaging, enabling the observation of individual platelet interactions and thrombus formation in real time. However, due to the standardization issues and relative novelty and complexity, microfluidic models are not yet as widely available in clinical settings as other methods such as ROTEM. While microfluidic models cannot be standardized to a "one-size-fits-all" solution, their versatility is at the same time a major benefit.

In summary, this systematic review underscores the versatility and potential of in vitro and ex vivo models in advancing our understanding of arterial thrombosis. These models are already an important tool in basic research and, with further standardization and advancements in technology, are likely to become essential tools in clinical practice as well.

Acknowledgment

The authors wish to thank Wichor Bramer from the Erasmus MC Medical Library for developing and updating the search strategies.

Statement of Ethics

A Statement of Ethics is not applicable because this study is based exclusively on published literature.

Conflict of Interest Statement

The authors have no conflict of interest to declare.

Funding Sources

This study was not supported by any sponsor or funder.

Author Contributions

Hande Eyisoylu and Rachele Cagnazzo contributed in conceptualization, methodology, writing-original draft, and preparation of figures. Gijsje H. Koenderink, Moniek P.M. de Maat, and Heleen M.M. van Beusekom contributed in conceptualization, supervision, and writing – review and editing.

Data Availability Statement

All data underlying the results are available as part of the article and the supplementary material, no additional data source is required.

References

1 Asada Y, Yamashita A, Sato Y, Hatakeyama K. Pathophysiology of atherothrombosis: mechanisms of thrombus formation on disrupted atherosclerotic plaques. Pathol Int. 2020;70(6):309–22. https://doi.org/10.1111/pin.12921

2 Davì G, Patrono C. Platelet activation and atherothrombosis. N Engl J Med. 2007;357(24):2482–94. https://doi.org/10.1056/nejmra071014

3 Karel MFA, Hechler B, Kuijpers MJE, Cosemans J. Atherosclerotic plaque injury-mediated murine thrombosis models: advantages and limitations. Platelets. 2020;31(4):439–46. https://doi.org/10.1080/09537104.2019.1708884

4 Westein E, de Witt S, Lamers M, Cosemans JM, Heemskerk JW. Monitoring in vitro thrombus formation with novel microfluidic devices. Platelets. 2012;23(7):501–9. https://doi.org/10.3109/09537104.2012.709653

5 Ayyoub S, Orriols R, Oliver E, Ceide OT. Thrombosis models: an overview of common in vivo and in vitro models of thrombosis. Int J Mol Sci. 2023;24(3):2569. https://doi.org/10.3390/ijms24032569

6 Cochrane A, Albers HJ, Passier R, Mummery CL, van den Berg A, Orlova VV, et al. Advanced in vitro models of vascular biology: human induced pluripotent stem cells and organ-on-chip technology. Adv Drug Deliv Rev. 2019;140:68–77. https://doi.org/10.1016/j.addr.2018.06.007

7 Mangin PH, Gardiner EE, Nesbitt WS, Kerrigan SW, Korin N, Lam WA, et al. In vitro flow based systems to study platelet function and thrombus formation: recommendations for standardization: communication from the SSC on Biorheology of the ISTH. J Thromb Haemost. 2020;18(3):748–52. https://doi.org/10.1111/jth.14717

8 Nesbitt WS, Mangin P, Salem HH, Jackson SP. The impact of blood rheology on the molecular and cellular events underlying arterial thrombosis. J Mol Med. 2006;84(12):989–95. https://doi.org/10.1007/s00109-006-0101-1

9 Dewey CF Jr., Bussolari SR, Gimbrone MA Jr., Davies PF. The dynamic response of vascular endothelial cells to fluid shear stress. J Biomech Eng. 1981;103(3):177–85. https://doi.org/10.1115/1.3138276

10 Hosseini V, Mallone A, Nasrollahi F, Ostrovidov S, Nasiri R, Mahmoodi M, et al. Healthy and diseased in vitro models of vascular systems. Lab Chip. 2021;21(4):641–59. https://doi.org/10.1039/d0lc00464b

11 Chandler AB. In vitro thrombotic coagulation of the blood; a method for producing a thrombus. Lab Invest. 1958;7(2):110–4.

12 Poole JC. A study of artificial thrombi produced by a modification of Chandler's method. Q J Exp Physiol Cogn Med Sci. 1959;44:377–84. https://doi.org/10.1113/expphysiol.1959.sp001419

13 Gardner RA. An examination of the fluid mechanics and thrombus formation time parameters in a Chandler rotating loop system. J Lab Clin Med. 1974;84(4):494–508.

14 Brubert J, Krajewski S, Wendel HP, Nair S, Stasiak J, Moggridge GD. Hemocompatibility of styrenic block copolymers for use in prosthetic heart valves. J Mater Sci Mater Med. 2016;27(2):32. https://doi.org/10.1007/s10856-015-5628-7

15 Monclova JL, Walsh DJ, Barraclough T, Hummel ME, Goetz I, Kannojiya V, et al. A hyper-viscoelastic uniaxial characterization of collagenous embolus analogs in acute ischemic stroke. J Mech Behav Biomed Mater. 2024;159:106690. https://doi.org/10.1016/j.jmbbm.2024.106690

16 Eyisoylu H, Hazekamp ED, Cruts J, Koenderink GH, de Maat MPM. Flow affects the structural and mechanical properties of the fibrin network in plasma clots. J Mater Sci Mater Med. 2024;35(1):8. https://doi.org/10.1007/s10856-024-06775-1

17 Christodoulides A, Hall AR, Umesh A, Alves NJ. Tracking fibrinolysis of Chandler loop-formed whole blood clots under shear flow in an in-vitro thrombolysis. Model. 2024.

18 Touma H, Sahin I, Gaamangwe T, Gorbet MB, Peterson SD. Numerical investigation of fluid flow in a Chandler loop. J Biomech Eng. 2014;136(7):071004. https://doi.org/10.1115/1.4027330

19 Booth NA, Simpson AJ, Croll A, Bennett B, MacGregor IR. Plasminogen activator inhibitor (PAI-1) in plasma and platelets. Br J Haematol. 1988;70(3):327–33. https://doi.org/10.1111/j.1365-2141.1988.tb02490.x

20 van Oeveren W, Tielliu IF, de Hart J. Comparison of modified chandler, roller pump, and ball valve circulation models for in vitro testing in high blood flow conditions: application in thrombogenicity testing of different materials for vascular applications. Int J Biomater. 2012;2012:673163. https://doi.org/10.1155/2012/673163

21 Baert EJ, Vandersteene J, Dewaele F, Vantilborgh A, Van Roost D, De Somer F. A new dynamic model for in vitro evaluation of intravascular devices. Int J Artif Organs. 2019;42(1):42–8. https://doi.org/10.1177/0391398818806158

22 Slee JB, Alferiev IS, Levy RJ, Stachelek SJ. The use of the ex vivo Chandler Loop apparatus to assess the biocompatibility of modified polymeric blood conduits. J Vis Exp. 2014(90):51871. https://doi.org/10.3791/51871

23 Zhang W, Li P, Neumann B, Haag H, Li M, Xu Z, et al. Chandler-Loop surveyed blood compatibility and dynamic blood triggered degradation behavior of Zn-4Cu alloy and Zn. Mater Sci Eng C Mater Biol Appl. 2021;119:111594. https://doi.org/10.1016/j.msec.2020.111594

24 Chin-Quee SL, Hsu SH, Nguyen-Ehrenreich KL, Tai JT, Abraham GM, Pacetti SD, et al. Endothelial cell recovery, acute thrombogenicity, and monocyte adhesion and activation on fluorinated copolymer and phosphorylcholine polymer stent coatings. Biomaterials. 2010;31(4):648–57. https://doi.org/10.1016/j.biomaterials.2009.09.079

25 Lev EI, Patel R, Karim A, Kleiman A, Badimon JJ, Kleiman NS. Anti-thrombotic effect of bivalirudin compared with eptifibatide and unfractionated heparin in diabetic patients: an ex vivo human study. Thromb Haemost. 2006;95(3):441–6. https://doi.org/10.1160/TH05-10-0700

26 Wåhlander K, Eriksson-Lepkowska M, Nyström P, Eriksson UG, Sarich TC, Badimon JJ, et al. Antithrombotic effects of ximelagatran plus acetylsalicylic acid (ASA) and clopidogrel plus ASA in a human ex vivo arterial thrombosis model. Thromb Haemost. 2006;95(03):447–53. https://doi.org/10.1160/th05-10-0664

27 Zafar U, Osende J, Shimbo D, Palencia S, Crook J, Leadley R, et al. Potent arterial antithrombotic effect of direct factor-Xa inhibition with ZK-807834 administered to coronary artery disease patients. Thromb Haemost. 2007;97(03):487–92. https://doi.org/10.1160/th06-04-0188

28 Zafar MU, Vorchheimer DA, Gaztanaga J, Velez M, Yadegar D, Moreno PR, et al. Antithrombotic effects of factor Xa inhibition with DU-176b: phase-I study of an oral, direct factor Xa inhibitor using an ex-vivo flow chamber. Thromb Haemost. 2007;98(4):883–8. https://doi.org/10.1160/th07-04-0312

29 Zafar MU, Santos-Gallego CG, Badimon L, Badimon JJ. Badimon perfusion chamber: an ex vivo model of thrombosis. Methods Mol Biol. 2018;1816:161–71. https://doi.org/10.1007/978-1-4939-8597-5_12

30 Lucking AJ, Chelliah R, Trotman AD, Connolly TM, Feuerstein GZ, Fox KA, et al. Characterisation and reproducibility of a human ex vivo model of thrombosis. Thromb Res. 2010;126(5):431–5. https://doi.org/10.1016/j.thromres.2010.06.030

31 Becker RC. A time-tested ex vivo model of thrombosis: from pathophysiology to drug development and disease application. Thromb Res. 2010;126(5):363–4. https://doi.org/10.1016/j.thromres.2010.08.023

32 Bossavy JP, Cadroy Y, Sakariassen K, Boneu B, Barret A. Nonfractionated heparin fails to inhibit arterial thrombosis in a human ex vivo thrombosis model. Ann Vasc Surg. 1999;13(4):393–401. https://doi.org/10.1007/s100169900274

33 Osende JI, Badimon JJ, Fuster V, Herson P, Rabito P, Vidhun R, et al. Blood thrombogenicity in type 2 diabetes mellitus patients is associated with glycemic control. J Am Coll Cardiol. 2001;38(5):1307–12. https://doi.org/10.1016/s0735-1097(01)01555-8

34 Badimon L, Badimon JJ, Galvez A, Turitto V, Fuster V. Platelet interaction with vessel wall and collagen in pigs with homozygous von Willebrand's disease associated with abnormal collagen aggregation. Thromb Haemost. 1989;61(01):057–64. https://doi.org/10.1055/s-0038-1646527
35 Glassberg J, Rahman AH, Zafar M, Cromwell C, Punzalan A, Badimon JJ, et al. Application of phospho-CyTOF to characterize immune activation in patients with sickle cell disease in an ex vivo model of thrombosis. J Immunol Methods. 2018;453:11–9. https://doi.org/10.1016/j.jim.2017.07.014
36 Badimon L, Badimon JJ, Galvez A, Chesebro JH, Fuster V. Influence of arterial damage and wall shear rate on platelet deposition. Ex vivo study in a swine model. Arteriosclerosis. 1986;6(3):312–20. https://doi.org/10.1161/01.atv.6.3.312
37 Badimon L, Badimon JJ. Mechanisms of arterial thrombosis in nonparallel streamlines: platelet thrombi grow on the apex of stenotic severely injured vessel wall. Experimental study in the pig model. J Clin Investig. 1989;84(4):1134–44. https://doi.org/10.1172/JCI114277
38 Fernández-Ortiz A, Badimon JJ, Falk E, Fuster V, Meyer B, Mailhac A, et al. Characterization of the relative thrombogenicity of atherosclerotic plaque components: implications for consequences of plaque rupture. J Am Coll Cardiol. 1994;23(7):1562–9. https://doi.org/10.1016/0735-1097(94)90657-2
39 Badimon L, Badimon JJ, Turitto VT, Fuster V. Role of von Willebrand factor in mediating platelet-vessel wall interaction at low shear rate; the importance of perfusion conditions. Blood. 1989;73(4):961–7. https://doi.org/10.1182/blood.v73.4.961.bloodjournal734961
40 Zafar MU, Ibáñez B, Choi BG, Vorchheimer DA, Piñero A, Jin X, et al. A new oral antiplatelet agent with potent antithrombotic properties: comparison of DZ-697b with clopidogrel a randomised phase I study. Thromb Haemost. 2010;103(1):205–12. https://doi.org/10.1160/TH09-06-0378
41 Zafar MU, Vilahur G, Choi BG, Ibanez B, Viles-Gonzalez JF, Salas E, et al. A novel antiischemic nitric oxide donor (LA419) reduces thrombogenesis in healthy human subjects. J Thromb Haemost. 2007;5(6):1195–200. https://doi.org/10.1111/j.1538-7836.2007.02543.x
42 Kim DA, Ku DN. Structure of shear-induced platelet aggregated clot formed in an in vitro arterial thrombosis model. Blood Adv. 2022;6(9):2872–83. https://doi.org/10.1182/bloodadvances.2021006248
43 Casa LD, Deaton DH, Ku DN. Role of high shear rate in thrombosis. J Vasc Surg. 2015;61(4):1068–80. https://doi.org/10.1016/j.jvs.2014.12.050
44 Hartert H. [Blood clotting studies with Thrombus stressography; a new Investigation procedure] Blutgerinnungsstudien mit der Thrombelastographie; einem neuen Untersuchungsverfahren. Klin Wochenschr. 1948;26(37–38):577–83. https://doi.org/10.1007/BF01697545
45 Whiting D, DiNardo JA. TEG and ROTEM: technology and clinical applications. Am J Hematol. 2014;89(2):228–32. https://doi.org/10.1002/ajh.23599
46 Nielsen VG. A comparison of the Thrombelastograph and the ROTEM. Blood Coagul Fibrinolysis. 2007;18(3):247–52. https://doi.org/10.1097/MBC.0b013e328092ee05
47 Budnik I, Shenkman B, Morozova O, Einav Y. Thromboelastometry assessment of the effects of fibrinogen, activated prothrombin complex concentrate, and tranexamic acid on clot formation and fibrinolysis in a model of trauma-induced coagulopathy. Eur J Trauma Emerg Surg. 2021;47(4):1057–63. https://doi.org/10.1007/s00068-019-01283-2
48 Govers-Riemslag JWP, Konings J, Cosemans J, van Geffen JP, de Laat B, Heemskerk JWM, et al. Impact of Deficiency of intrinsic coagulation factors XI and XII on ex vivo thrombus formation and clot lysis. TH Open. 2019;3(3):e273–e285. https://doi.org/10.1055/s-0039-1693485
49 Samoš M, Škorňová I, Bolek T, Stančiaková L, Korpallová B, Galajda P, et al. Viscoelastic Hemostatic assays and platelet function testing in patients with atherosclerotic vascular diseases. Diagnostics. 2021;11(1):143. https://doi.org/10.3390/diagnostics11010143
50 Sharma S, Farrington K, Kozarski R, Christopoulos C, Niespialowska-Steuden M, Moffat D, et al. Impaired thrombolysis: a novel cardiovascular risk factor in end-stage renal disease. Eur Heart J. 2013;34(5):354–63. https://doi.org/10.1093/eurheartj/ehs300
51 Yamamoto J, Inoue N, Otsui K, Ikarugi H, Shimizu M, Yamamoto S, et al. A point-of-care global thrombosis test measuring occlusion time and endogenous lysis time may indicate thrombotic status. Future Sci OA. 2019;5(6):Fso402. https://doi.org/10.2144/fsoa-2019-0052
52 Taomoto K, Ohnishi H, Kuga Y, Nakashima K, Ichioka T, Kodama Y, et al. Platelet function and spontaneous thrombolytic activity of patients with cerebral infarction assessed by the global thrombosis test. Pathophysiol Haemost Thromb. 2010;37(1):43–8. https://doi.org/10.1159/000315494
53 Kanji R, Leader J, Memtsas V, Gorog DA. Measuring thrombus stability at high shear, together with thrombus formation and endogenous fibrinolysis: first experience using the global thrombosis test 3 (GTT-3). Clin Appl Thromb Hemost. 2023;29:10760296231181917. https://doi.org/10.1177/10760296231181917
54 Otsui K, Gorog DA, Yamamoto J, Yoshioka T, Iwata S, Suzuki A, et al. Global Thrombosis test - a possible monitoring system for the effects and safety of dabigatran. Thromb J. 2015;13:39. https://doi.org/10.1186/s12959-015-0069-6
55 Clavería V, Yang PJ, Griffin MT, Ku DN. Global thrombosis test: occlusion by coagulation or SIPA? TH Open. 2021;5(3):e400–e10.
56 Yamamoto J, Ijiri Y, Ikarugi H, Otsui K, Inoue N, Sakariassen KS. Prevention of thrombotic disorders by antithrombotic diet and exercise: evidence by using global thrombosis tests. Future Sci OA. 2018;4(4):Fso285. https://doi.org/10.4155/fsoa-2017-0104
57 Murakami M, Otsui K, Ijiri Y, Shimizu M, Ikarugi H, Shioyama W, et al. Global thrombosis test for assessing thrombotic status and efficacy of antithrombotic diet and other conditions. Future Sci OA. 2022;8(3):Fso788. https://doi.org/10.2144/fsoa-2021-0086
58 Duffy DC, McDonald JC, Schueller OJ, Whitesides GM. Rapid Prototyping of microfluidic systems in Poly(dimethylsiloxane). Anal Chem. 1998;70(23):4974–84. https://doi.org/10.1021/ac980656z
59 Cosemans JM, Kuijpers MJ, Lecut C, Loubele ST, Heeneman S, Jandrot-Perrus M, et al. Contribution of platelet glycoprotein VI to the thrombogenic effect of collagens in fibrous atherosclerotic lesions. Atherosclerosis. 2005;181(1):19–27. https://doi.org/10.1016/j.atherosclerosis.2004.12.037
60 Karel MFA, Lemmens TP, Tullemans BME, Wielders SJH, Gubbins E, van Beurden D, et al. Characterization of atherosclerotic plaque coating for thrombosis microfluidics assays. Cell mol bioeng. 2022;15(1):55–65. https://doi.org/10.1007/s12195-021-00713-9
61 Berry J, Peaudecerf FJ, Masters NA, Neeves KB, Goldstein RE, Harper MT. An "occlusive thrombosis-on-a-chip" microfluidic device for investigating the effect of anti-thrombotic drugs. Lab Chip. 2021;21(21):4104–17. https://doi.org/10.1039/d1lc00347j
62 Cadroy Y, Sakariassen K, Grandjean H, Thalamas C, Boneu B, Sié P. The effect of platelet PlA polymorphism on experimental thrombus formation in man depends on blood flow and thrombogenic substrate. Thromb Haemost. 2001;85(06):1097–103. https://doi.org/10.1055/s-0037-1615972
63 Walton BL, Lehmann M, Skorczewski T, Holle LA, Beckman JD, Cribb JA, et al. Elevated hematocrit enhances platelet accumulation following vascular injury. Blood. 2017;129(18):2537–46. https://doi.org/10.1182/blood-2016-10-746479
64 Vignoli A, Gamba S, van der Meijden PEJ, Marchetti M, Russo L, Tessarolo S, et al. Increased platelet thrombus formation under flow conditions in whole blood from polycythaemia vera patients. Blood Transfus. 2022;20(2):143–51. https://doi.org/10.2450/2021.0456-20
65 Yue M, Luo D, Yu S, Liu P, Zhou Q, Hu M, et al. Misshapen/NIK-related kinase (MINK1) is involved in platelet function, hemostasis, and thrombus formation. Blood. 2016;127(7):927–37. https://doi.org/10.1182/blood-2015-07-659185

66 Westein E, van der Meer AD, Kuijpers MJ, Frimat JP, van den Berg A, Heemskerk JW. Atherosclerotic geometries exacerbate pathological thrombus formation post-stenosis in a von Willebrand factor-dependent manner. Proc Natl Acad Sci U S A. 2013;110(4):1357–62. https://doi.org/10.1073/pnas.1209905110
67 Cho M, Park JK. Modular 3D in vitro artery-mimicking Multichannel system for recapitulating vascular stenosis and inflammation. Micromachines (Basel). 2021;12(12):1528. https://doi.org/10.3390/mi12121528
68 Mangin PH, Neeves KB, Lam WA, Cosemans J, Korin N, Kerrigan SW, et al. In vitro flow-based assay: from simple toward more sophisticated models for mimicking hemostasis and thrombosis. J Thromb Haemost. 2021;19(2):582–7. https://doi.org/10.1111/jth.15143
69 Pandian NKR, Mannino RG, Lam WA, Jain A. Thrombosis-on-a-chip: prospective impact of microphysiological models of vascular thrombosis. Curr Opin Biomed Eng. 2018;5:29–34. https://doi.org/10.1016/j.cobme.2017.12.001
70 Karel MFA, Tullemans BME, D'Italia G, Lemmens TP, Claushuis TAM, Kuijpers MJE, et al. The effect of Bruton's tyrosine kinase inhibitor ibrutinib on atherothrombus formation under stenotic flow conditions. Thromb Res. 2022;212:72–80. https://doi.org/10.1016/j.thromres.2022.02.020
71 Penz S, Reininger AJ, Brandl R, Goyal P, Rabie T, Bernlochner I, et al. Human atheromatous plaques stimulate thrombus formation by activating platelet glycoprotein VI. The FASEB J. 2005;19(8):898–909. https://doi.org/10.1096/fj.04-2748com
72 Qiu Y, Lin J, Wang A, Fang Z, Sakurai Y, Choi H, et al. Clinically relevant clot resolution via a thromboinflammation-on-a-chip. Nature. 2025;641(8065):1298–308. https://doi.org/10.1038/s41586-025-08804-7
73 Costa PF, Albers HJ, Linssen JEA, Middelkamp HHT, van der Hout L, Passier R, et al. Mimicking arterial thrombosis in a 3D-printed microfluidic in vitro vascular model based on computed tomography angiography data. Lab Chip. 2017;17(16):2785–92. https://doi.org/10.1039/c7lc00202e
74 Lui M, Gardiner EE, Arthur JF, Pinar I, Lee WM, Ryan K, et al. Novel stenotic microchannels to study thrombus formation in shear gradients: influence of shear forces and human platelet-related factors. Int J Mol Sci. 2019;20(12):2967. https://doi.org/10.3390/ijms20122967
75 Colace TV, Muthard RW, Diamond SL. Thrombus growth and embolism on tissue factor-bearing collagen surfaces under flow: role of thrombin with and without fibrin. Arterioscler Thromb Vasc Biol. 2012;32(6):1466–76. https://doi.org/10.1161/ATVBAHA.112.249789
76 Li M, Hotaling NA, Ku DN, Forest CR. Microfluidic thrombosis under multiple shear rates and antiplatelet therapy doses. PLoS One. 2014;9(1):e82493. https://doi.org/10.1371/journal.pone.0082493
77 Akther F, Zhang J, Tran HDN, Fallahi H, Adelnia H, Phan H-P, et al. Atherothrombosis-on-Chip: a site-specific microfluidic model for thrombus formation and drug Discovery. Adv Biol. 2022;6(7):2101316. https://doi.org/10.1002/adbi.202101316
78 Gao X, Zhang T, Huang X, Huan X, Li Y. Impact of rise and fall phases of shear on platelet activation and aggregation using microfluidics. J Thromb Thrombolysis. 2024;57(4):576–86. https://doi.org/10.1007/s11239-024-02968-1
79 Watson CT, Ward SC, Rizzo SA, Redaelli A, Manning KB. Influence of hematocrit level and integrin $\alpha_{IIb}\beta_{III}$ function on vWF-mediated platelet adhesion and shear-induced platelet aggregation in a sudden expansion. Cel Mol Bioeng. 2024;17(1):49–65. https://doi.org/10.1007/s12195-024-00796-0
80 Colace TV, Tormoen GW, McCarty OJ, Diamond SL. Microfluidics and coagulation biology. Annu Rev Biomed Eng. 2013;15:283–303. https://doi.org/10.1146/annurev-bioeng-071812-152406
81 Muthard RW, Diamond SL. Blood clots are rapidly assembled hemodynamic sensors: flow arrest triggers intraluminal thrombus contraction. Thromb Vasc Biol. 2012;32(12):2938–45. https://doi.org/10.1161/ATVBAHA.112.300312
82 Yamamoto J, Inoue N, Otsui K, Ishii H, Gorog DA. Global Thrombosis test (GTT) can detect major determinants of haemostasis including platelet reactivity, endogenous fibrinolytic and thrombin generating potential. Thromb Res. 2014;133(5):919–26. https://doi.org/10.1016/j.thromres.2014.02.018
83 Bark DL, Vital EF, Oury C, Lam WA, Gardiner EE. Recommendations for defining disturbed flow as laminar, transitional, or turbulent in assays of hemostasis and thrombosis: communication from the ISTH SSC Subcommittee on Biorheology. J Thromb Haemost. 2025;23(1):345–58. https://doi.org/10.1016/j.jtha.2024.09.026
84 Cadroy Y, Pillard F, Sakariassen KS, Thalamas C, Boneu B, Riviere D. Strenuous but not moderate exercise increases the thrombotic tendency in healthy sedentary male volunteers. J Appl Physiol. 2002;93(3):829–33. https://doi.org/10.1152/japplphysiol.00206.2002
85 Deng YJ, Duque JA, Su CX, Zhou YQ, Nishikawa M, Xiao TH, et al. Understanding stenosis-induced platelet aggregation on a chip by high-speed optical imaging. Sens Actuator B-Chem. 2022;356:131318. https://doi.org/10.1016/j.snb.2021.131318
86 Casa LDC, Ku DN. Geometric design of microfluidic chambers: platelet adhesion versus accumulation. Biomed Microdevices. 2014;16(1):115–26. https://doi.org/10.1007/s10544-013-9811-7
87 Griffin MT, Kim D, Ku DN. Shear-induced platelet aggregation: 3D-grayscale microfluidics for repeatable and localized occlusive thrombosis. Biomicrofluidics. 2019;13(5):054106. https://doi.org/10.1063/1.5113508
88 Roest M, Reininger A, Zwaginga JJ, King MR, Heemskerk JW, Biorheology Sub, committee of the SSC of the ISTH. Flow chamber-based assays to measure thrombus formation in vitro: requirements for standardization. J Thromb Haemost. 2011;9(11):2322–4. https://doi.org/10.1111/j.1538-7836.2011.04492.x
89 McCarty OJT, Ku D, Sugimoto M, King MR, Cosemans JMEM, Neeves KB, et al. Dimensional analysis and scaling relevant to flow models of thrombus formation: communication from the SSC of the ISTH. J Thromb Haemost. 2016;14(3):619–22. https://doi.org/10.1111/jth.13241
90 Ayyoub S, Orriols R, Oliver E, Ceide OT. Thrombosis models: an overview of common in vivo and in vitro models of thrombosis. Int J Mol Sci. 2023;24(3):2569. https://doi.org/10.3390/ijms24032569
91 Marcial HBF, Choi J, Ham D, Kim J, Jeong P, Choi J, et al. Influence of multiple stenoses on thrombosis formation: an in vitro study. Micro Nano Syst Lett. 2022;10(1):18. https://doi.org/10.1186/s40486-022-00159-2
92 Brinkman H, Zuurveld M, Meijers J. Factor V as adjunct to fibrinogen and prothrombin complex concentrate in an in vitro model of combined severe trauma-induced coagulopathy and rivaroxaban anticoagulation. In: Abstracts from the ISTH 2023 Congress, Jun 24–28, 2023, Montreal, Canada. Res Pract Thromb Haemost. 2023;7:PB1313.
93 Jain A, van der Meer AD, Papa A-L, Barrile R, Lai A, Schlechter BL, et al. Assessment of whole blood thrombosis in a microfluidic device lined by fixed human endothelium. Biomed Microdevices. 2016;18(4):73. https://doi.org/10.1007/s10544-016-0095-6
94 Nguyen TQ, Park W-T. Fabrication method of multi-depth circular microchannels for investigating arterial thrombosis-on-a-chip. Sens Actuator B-Chem. 2020;321:128590.
95 van Rooij BJM, Závodszky G, Hoekstra AG, Ku DN. Biorheology of occlusive thrombi formation under high shear: in vitro growth and shrinkage. Sci Rep. 2020;10(1):18604. https://doi.org/10.1038/s41598-020-74518-7
96 Tsai M, Kita A, Leach J, Rounsevell R, Huang JN, Moake J, et al. In vitro modeling of the microvascular occlusion and thrombosis that occur in hematologic diseases using microfluidic technology. J Clin Invest. 2012;122(1):408–18. https://doi.org/10.1172/JCI58753
97 Belenkovich M, Veksler R, Kreinin Y, Mekler T, Flores M, Sznitman J, et al. Clot accumulation in 3D microfluidic bifurcating microvasculature network. Micromachines. 2024;15(8):988. https://doi.org/10.3390/mi15080988